SEMARAK ILMU PUBLISHING

Journal of Advanced Research in Fluid Mechanics and Thermal Sciences

Journal homepage:
https://semarakilmu.com.my/journals/index.php/fluid_mechanics_thermal_sciences/index
ISSN: 2289-7879

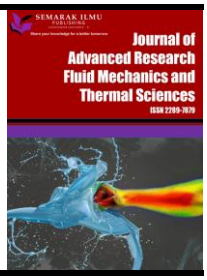

Numerical Predictions of Laminar Free and Mixed Convection Heat Transfer to Supercritical Water from a Non-Isothermal Vertical Plate

Rajendra Prasad Keralapura Suresh[1,*], Seetharam Tirumkudlu Ramarao[2]

[1] Manipal Institute of Technology Bengaluru, Manipal Academy of Higher Education, Manipal, India
[2] Process Modelling Research Laboratory, PES University Bangalore, India

ARTICLE INFO

Article history:
Received 18 January 2023
Received in revised form 9 May 2023
Accepted 14 May 2023
Available online 29 May 2023

Keywords:
Supercritical water; mixed convection; free convection, non-isothermal wall; vertical surface; near-critical fluid

ABSTRACT

Numerical predictions of heat transfer have been made for laminar free and mixed convective heat transfer from non-isothermal vertical plane surface to supercritical water. Variation of all the thermo-physical properties of the supercritical fluid under investigation have been considered. The numerical scheme employed in the present investigation is first validated with respect to experimental data for isothermal wall conditions and good agreement is achieved with maximum deviation not exceeding 15 %. Linear and parabolic variation of wall temperatures are considered for the present investigation. Computations are made for two pressures of 225 Bar and 235 Bar, for wide range of temperature difference from 4K to 20K. The values of temperature difference are chosen. Based on the results obtained, correlations have been proposed to evaluate the Nusselt numbers for both free and mixed convection with pressure ratios of P/P_c = 1.02 (p = 225 bar) and P/P_c = 1.065 (p = 235 bar). The correlations cover a range of Rayleigh numbers, Ra_x from 10^6 to 10^9 for Free Convection and grashoff Number/Reynolds Number^2 ranging from 0.4 to 8 for Mixed convection. The proposed correlations for local Nusselt numbers do not exceed maximum deviation of 15% from the predicted values. It has been found that the maximum deviation occurs for those cases for which the pseudo-critical temperature, T^* is within the boundary layer. It is further observed that for these cases both the velocity and temperature profiles are distorted at locations where the temperature is close to the pseudo-critical temperature thereby affecting the gradients at the wall, which in turn influences the heat transfer coefficient.

1. Introduction

Heat transfer problems can be divided in into four regimes: gaseous, liquid, two-phase and near critical. Supercritical fluids (fluids in the near critical region) can be termed as fluids which do not possess two distinct phases above a certain temperature and above a certain pressure [1]. The necessity of a comprehensive study on heat transfer in fluids beyond their critical temperature and pressure is of a great scope in recent times due to their extensive applications in numerous fields. Supercritical water is utilized in multidisciplinary areas like oxidation, hydrolysis, gasification, power

* *Corresponding author.*
E-mail address: rajendra.prasad@manipal.edu

https://doi.org/10.37934/arfmts.106.2.2253

generation and many more. Fluids like carbon dioxide, helium and nitrogen in the near critical region also have been used in many industrial applications. Kakac [2], Polyakov [3], and Hall [4] have reported that, the studies on the problem of free convection to the supercritical fluids have been very complex due to the severe variation of various thermophysical properties in the near critical region, especially near the pseudo-critical temperature, T^*. Numerous experiments have been carried out, considering carbon dioxide, water and helium as the primary working fluids.

The variation of thermophysical properties (c_p, k, μ and ρ) of water at three different supercritical pressures, namely 225 bar, 235 bar and 245 bar are obtained from NIST thermo-physical database [5] and plotted as shown in Figure 1 to Figure 4. It can be observed from these figures, the severe variation of the properties, which are generally non-linear in nature, occur at temperatures close to T^*. and this type of variation of the properties make the governing equations nonlinear and this poses additional difficulty in solving these equations. Figure 1 shows that for 225 bar c_p varies by a factor 14 near T^*, whereas for 245 bars, the factor reduces to about 5.

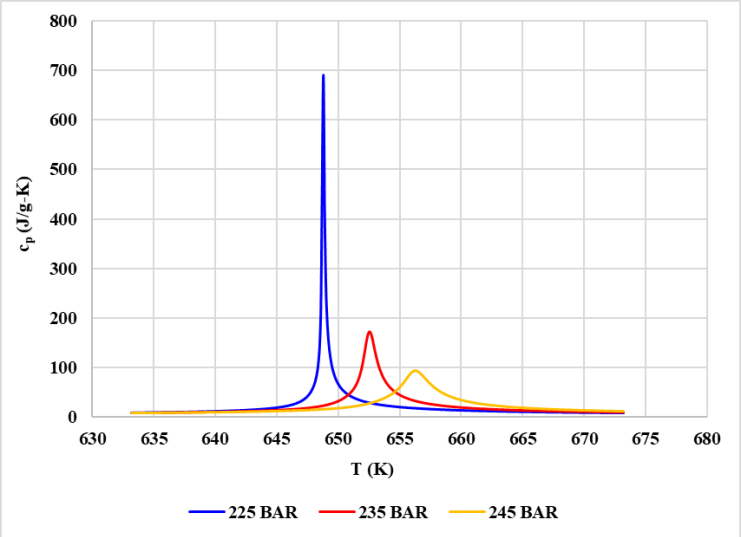

Fig. 1. Variation of c_p with respect to temperature and pressure for water

Figure 2 indicates that there is a significant spike in the value of k near T^* for 225 bars, whereas the spike becomes insignificant for 245 bars.

The thermal conductivity shown in Figure 3 and Figure 4 show that, there are no spikes in the values of viscosity and density, but there is steep reduction in their values near T^*. It has been established by almost all the earlier investigators, that the correlations to calculate the heat transfer coefficients, based on constant property solutions are significantly different from the experimental data for near-critical fluids. It is therefore necessary to solve the governing equations for supercritical fluids, taking into account the actual variation of all the required fluid properties.

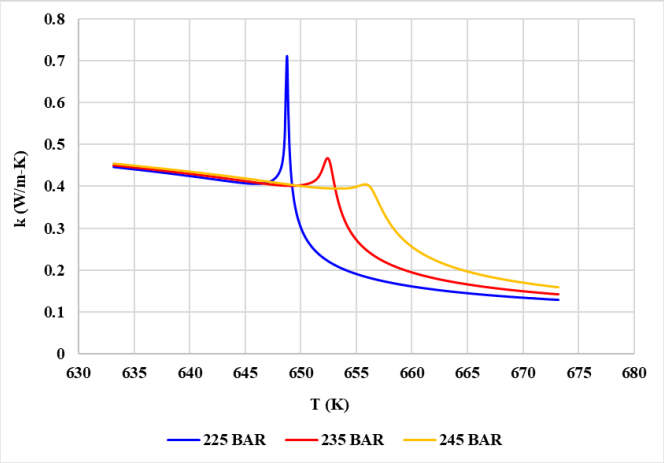

Fig. 2. Variation of *k* with respect to temperature and pressure for water

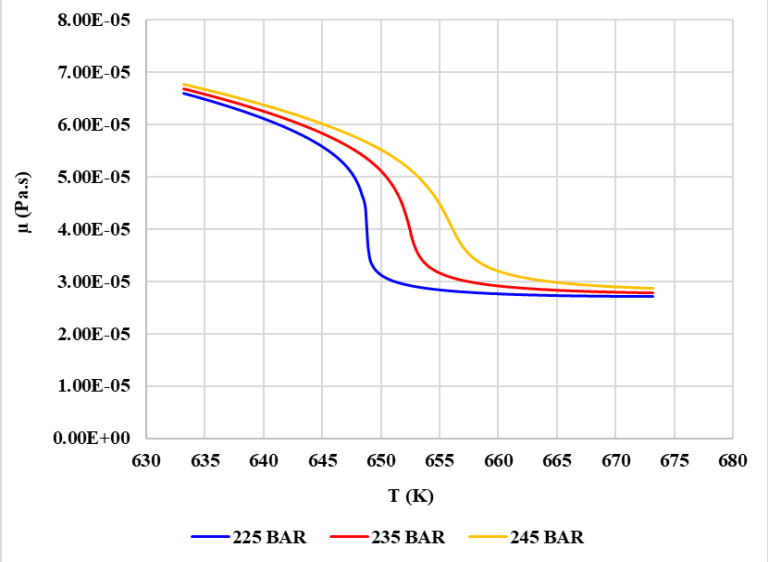

Fig. 3. Variation of μ with respect to temperature and pressure for water

A number of investigations (theoretical and experimental) on the problem of free convection to supercritical fluids [6-10] have been reported in literature. Almost all theoretical investigations [6-10] are carried out either by using principle of similarity or using integral method to solve the governing equations. In all these cases, the values of ΔT ($\Delta T = T_w - T_\infty$) is less than 16 K.

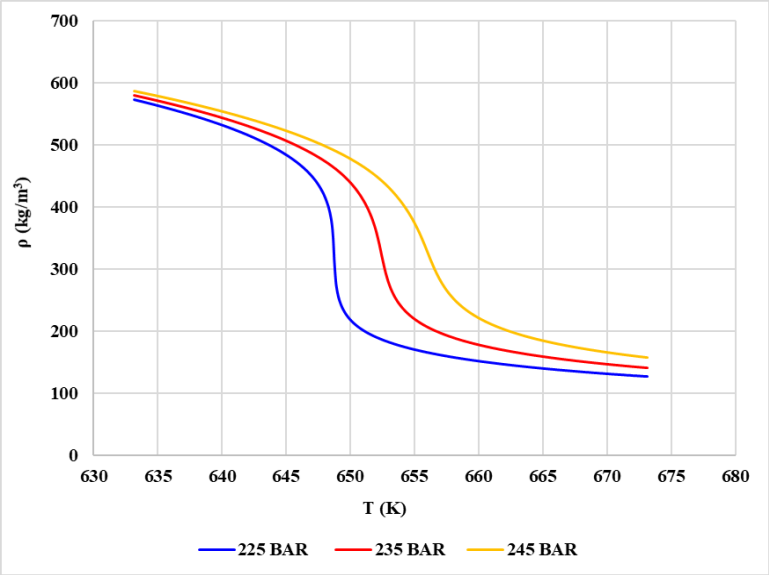

Fig. 4. Variation of ρ with respect to temperature and pressure for water

Seetharam and Sharma [11,12] have numerically solved the problem of laminar free convective heat transfer from a plane vertical surface to carbon dioxide (P/P_c= 1.02 to 1.35) and water (P/P_c= 1.02 to 1.11) in the near critical region using Patankar-Spalding implicit finite different scheme [11-12] with suitable modifications to account for the severe variation of the all the required properties of the fluid. They have also proposed correlations for local Nusselt number. Their investigation is restricted to uniform heat flux (q_w=1000 W/m^2 to 50000 W/m^2) and constant wall temperature ($\Delta T \leq$ 20K) boundary conditions. Seetharam and Sharma [13] have also investigated the problem of turbulent free convection from a plane vertical surface with uniform wall heat flux (q_w= 1000 W/m^2 to 25000 W/m^2) to supercritical carbon dioxide at 75 Bar.

In the literature, the problem of forced and mixed convective heat transfer to near critical fluids from vertical plane surface is sparse. Boundary layer velocity as well as temperature profiles have been determined in the turbulent flow regime for forced convective heat transfer to supercritical nitrogen from a plane isothermal vertical surface [14]. Seetharam *et.al.,* [15] have numerically solved the problem of laminar forced and mixed convection heat transfer from a plane vertical isothermal surface ($\Delta T \leq$ 30K) to supercritical carbon dioxide (P/P_c= 1.02 to 1.35) using the modified Spalding and Patankar implicit FDM [11,12]. They have investigated both aiding flow and opposing flow situations.

Very little information is available on the problem of free convection to supercritical fluids from plane vertical surfaces with non-uniform wall temperature or non-uniform heat flux conditions Teymourtash and Ebrahimi Warkiani [16] have investigated numerically, the problem of laminar free convection with uniform or non-uniform prescribed wall temperature (linear variation) and Teymourtash *et al.,* [17] have investigated the problem of free convection for vertical flat plate with uniform or non-uniform prescribed wall heat flux (linear variation) to a supercritical fluid. For both the problems, the authors have derived a new equation for thermal expansion coefficient in a supercritical fluid based on Redlich–Kwong [21] equation of state, as a function of pressure, temperature, and the compressibility factor. Calculated values of thermal expansion coefficient have been compared with the experimental results which show better accuracy in comparison with van der Waals equation of state. The governing systems of partial differential equations were solved numerically using the finite difference method. The local Nusselt number was calculated and plotted as a function of the local Rayleigh number. Using supercritical fluids in constant heat flux free

convection, decrease the wall temperature in comparison with sub critical fluids. It is observed that positive and negative slopes of surface heat flux distribution increases and decreases the heat transfer coefficient respectively. In the linear wall temperature case, they have found that a positive slope of temperature distribution ($dT_w/dx > 0$) will increase the heat transfer rate, and a negative one ($dT_w/dx < 0$) will decrease the heat transfer rate.

In both the investigations the authors have assumed that Boussinesq approximation is completely valid, by stating that for the supercritical condition far from the critical point with more temperature differences, the Boussinesq approximation is completely valid. In addition, they have assumed that the other fluid properties, namely fluid viscosity, thermal conductivity and specific heat at constant pressure are constants in the flow field. These assumptions are not valid for fluids in the near critical region, especially for pressures close to critical pressure and temperatures in the flow field, is in the neighbourhood of T*. They have obtained solutions for carbon dioxide for p = 110.7 bar ($p/p_{cr} = 1.5$) where the property variation is not very severe and hence their solutions seem to be valid using Boussinesq approximation. They could not compare their predictions with experimental data as no such data is available, but compared their predictions with correlation proposed by Churchill and Chu [22] which is based on predictions for constant property fluids, to know how far their predictions deviate from the correlation proposed by Churchill and Chu [22]. It should be pointed out that, whether, their solution using Boussinesq approximation is valid for pressures close to critical pressure ($p/p_{cr} \leq 1.4$ for carbon dioxide) and temperatures in the neighbourhood of T*. The velocity and temperature profiles presented by them do not indicate any distortion, whereas Seetharam and Sharma [8] have predicted that, whenever T* lies within the boundary layer, distortion of the profiles occur and hence affect the velocity and temperature gradient at the wall, thereby influencing the drag coefficient and Nusselt number respectively. From this comparison, it can be concluded that the cases studied by Teymourtash and Ebrahimi Warkiani [16] and Teymourtash *et al.,* [17], T* did not lie within the boundary layer. They have not proposed any correlation to predict the heat transfer coefficient. Further Basha *et al.,* [20] carried out thermodynamic analysis of natural convection supercritical water flow past a stretching sheet and concluded that the RK-EOS is the suitable method to find convection properties. Using the developed EOS approach Basha *et al.,* [21] were successful in the analysis of supercritical free convection in Newtonian and couple stress fluids. Basha *et al.,* [22] have also contributed to find heat transfer characteristics of supercritical nitrogen using the Redlich-kwong equation of state.

Regardless of lot of research in this area, there is a need for accurate investigations on the problems of free, forced, and mixed convective heat transfer to near critical fluids from plane vertical surfaces with varying wall temperature and varying wall heat flux conditions.

In the present investigation, numerical predictions have been made for free and mixed convective heat transfer to supercritical water from a plane vertical non-isothermal surface. Linear surface temperature variation and parabolic variation of surface temperature are chosen for two supercritical pressures of water (225 Bar and 235 Bar). Based on the results obtained, a correlation to determine the local Nusselt number is proposed for each case.

2. Problem Statement

Buoyancy-driven convection to supercritical water over a vertical plate with variable wall temperature is considered for investigation. Steady, two-dimensional laminar boundary layer flow with negligible viscous dissipation is assumed. Numerical predictions are made using the CFD package FLUENT.

2.1 Physical Model

Figure 5 represents a two-dimensional rectangular plate with acceleration due to gravity in the negative x direction (g= -9.81 m/s^2). Top and bottom walls are insulated (zero heat flux). Walls are solid and subjected to no slip boundary conditions (zero velocity components). The plate acts as a 2-D vertical plane surface (with no porosity) in x-y plane. The length of the wall varies for different wall temperatures (T_w) as the study is confined to laminar flow of the fluid. The effective length of the wall till which the fluid remains laminar also varies for various non-isothermal walls (with different values of ΔT_L). Beyond the effective length of the wall, the fluid becomes turbulent.

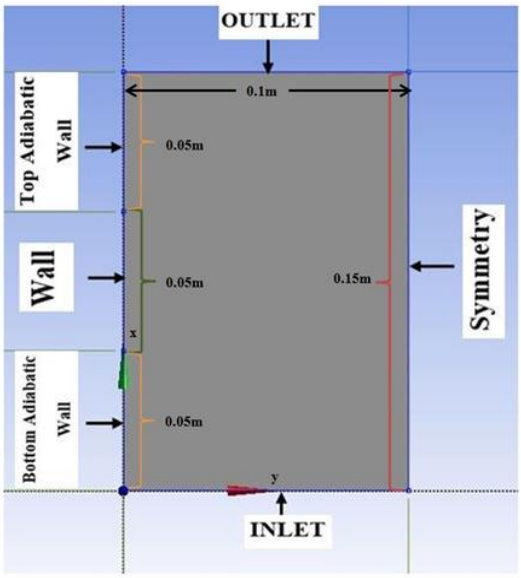

Fig. 5. Rectangular 2D vertical plane surface

2.2 Meshing

Figure 6 represents the structured fine mesh of vertical plate with 82511 elements. Mesh is refined with the face refinement option. All triangular elements are converted to quad elements to ensure uniform corner angle.

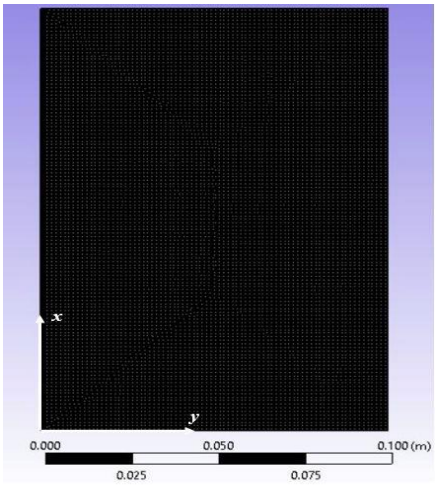

Fig. 6. Mesh configuration of plate

Figure 7 represents mesh inflation in the near wall region to ensure an effective boundary layer mesh with greater number of elements. The average orthogonal quality was found to be as high as 0.9997 and average skewness was as low as 3.275e-003.

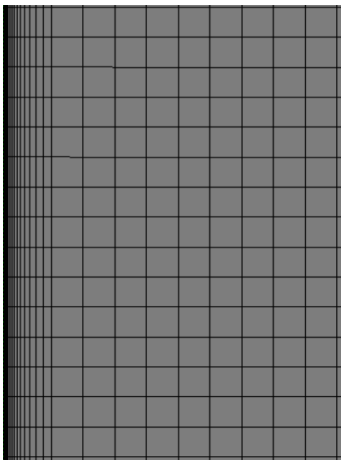

Fig. 7. Mesh in the near wall region

Grid independence study was carried out for free and mixed convection cases (P/P_c= 1.02) with non-isothermal walls, Nusselt number with respect to *x* was computed for 3 mesh sizes of 57507 elements, 82511 elements and 107503 elements. Based on the study, mesh size of 82511 elements is selected, as the error for Nu_x with respect to other mesh sizes did not exceed $\pm$1%. Mesh size of 107503 elements showcased significantly higher computing time. Also, based on mesh studies for isothermal formulation from an existing literature [10], a mesh with 82511 elements is selected as the most appropriate mesh size, as results are validated for the same fluid (supercritical water) at the same pressures (225 Bar and 235 Bar) and similar boundary conditions (T_∞=643.16K and ΔT up to 20K).

2.3 Numerical Method

The numerical analysis is carried out with computational fluid dynamics method of solving, where FLUENT is employed. FLUENT is a computational fluid dynamics software package that contains the extensive physical modelling abilities essential for modelling supercritical fluid flow and enhance heat transfer. Thermophysical property variations are taken into consideration and fed into the model. All the required properties are taken from NIST [5] and polynomials are fitted which give properties at any desired temperature which are within $\pm$1% from the NIST data.

2.4 Validation of Numerical Predictions with Experimental Data

The numerical method used in the present investigation is first validated with respect to experimental data of Fritsch and Grosh [6] for laminar free convection from plane vertical isothermal surface to supercritical water, since no experimental data is available for variable wall temperature conditions, Table 1 shows the comparison of numerically predicted surface heat flux variation with ΔT at a particular location (x = 0.3 m) with available experimental data for a pressure of 234.5 Bar (T^* =652.32 K) at three different average values of T_∞. It can be concluded from Table 1 that, for most of the cases studied, the maximum deviation does not exceed $\pm$15 % and the numerically predicted valuesof surface heat flux is comparatively higher than those obtained by experiments. The deviation

may be attributed to experimental errors and also to the different sources used to obtain the properties of supercritical water at this pressure (P = 234.5 Bar).

Table 1
Validation of numerical results with experimental data of Fritsch and Grosh [6]

SL No	T_∞ (K)	ΔT (K)	q_{Num}(W/m^2)	q_{Exp}(W/m^2)	Error (%)
1	651.50	1.71	3264.29	3265.00	-0.02
2	651.44	2.77	5307.19	5088.35	4.30
3	651.49	4.04	7360.79	7126.22	3.29
4	651.48	5.41	9099.36	8769.76	3.76
5	651.52	6.27	9715.19	9738.22	-0.24
6	651.57	6.91	10576.68	10574.19	0.02
7	652.12	1.80	3164.40	2757.11	14.77
8	652.05	3.62	5836.71	5050.50	15.57
9	651.98	5.58	8445.96	7340.73	15.06
10	651.99	6.59	9470.11	8321.81	13.80
11	652.03	7.87	10472.79	9574.18	9.39
12	652.13	8.51	11873.03	10552.10	12.52
13	652.04	1.88	2433.93	2230.30	9.13
14	652.38	2.84	3995.79	3482.67	14.73
15	652.11	3.21	4789.04	4255.54	12.54
16	652.09	4.77	6869.30	6119.90	12.25
17	652.37	6.68	8223.05	7239.78	13.58
18	652.12	7.61	10026.37	8990.58	11.52

To know the exact nature of variation of surface heat flux with respect to ΔT the tabulated values are shown graphically in Figure 8 to Figure 10. It is observed from these figures that the nature of variation is similar for both experimental and numerical investigations. It should be noted that Figure 10 shows a variation different from those indicated in Figure 8 and Figure 9, but similar to the experimental predictions.

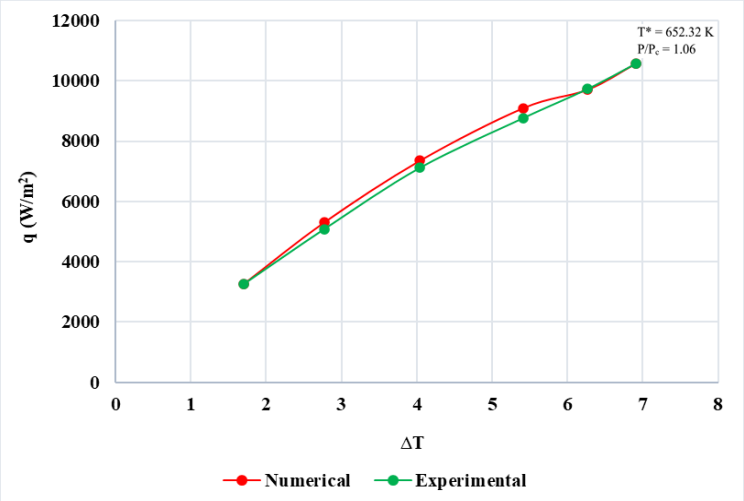

Fig. 8. Variation of q with ΔT for average T_∞= 651.50 Kat x = 0.3 m for 234.5 Bar

This is due to the fact that in all the cases shown in Figure 8 and Figure 9, T* lies outside the thermal boundary layer, whereas in Figure 10 for data points 14 and 17 in Table 1, the pseudo critical temperature T* lies inside the thermal boundary layer, whereas for the remaining data points, *T** lies outside the thermal boundary layer. Based on this comparison it was concluded that the numerical scheme used for validation can also be used for the present investigation.

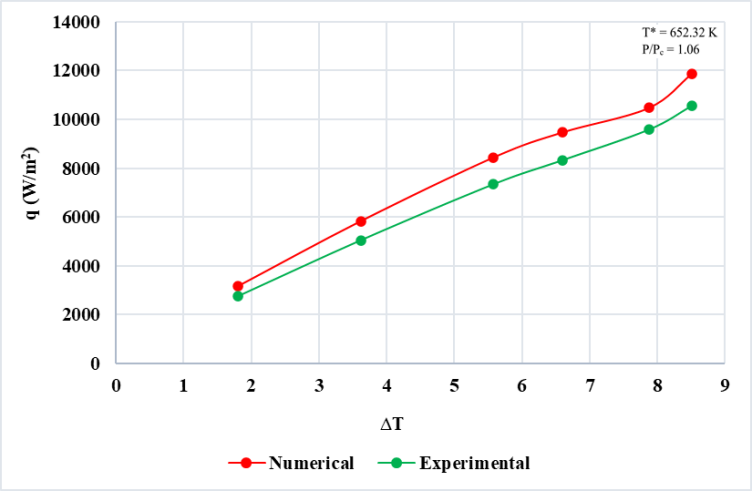

Fig. 9. Variation of *q* with *ΔT* for average T_∞= 652.05 K at*x* = 0.3 mfor 234.5 Bar

The present study is a laminar steady state 2D planar formulation with buoyancy driven aiding flow (T_w>T_∞). Pressure based solver is employed for the current work, where the primary variables remain pressure and momentum and a cell-based approach is used to solve the governing equations. SIMPLEC algorithm is implemented for velocity and pressure coupling. PRESTO is selected as the interpolation scheme for determining cell-face pressures. The upwind scheme of the second order is applied for the discretization of equations. To obtain a well converged solution, the under-relaxation factors for the energy and density are reduced to 0.8 from 1 (default value) to smoothen the variation in temperature and its dependent properties in between iterations. The absolute convergence criterion for the present simulation is that the RMS residual values must be less than 10^{-7} for energy and for the other variables like continuity; the RMS residuals should be less than 10^{-4}.

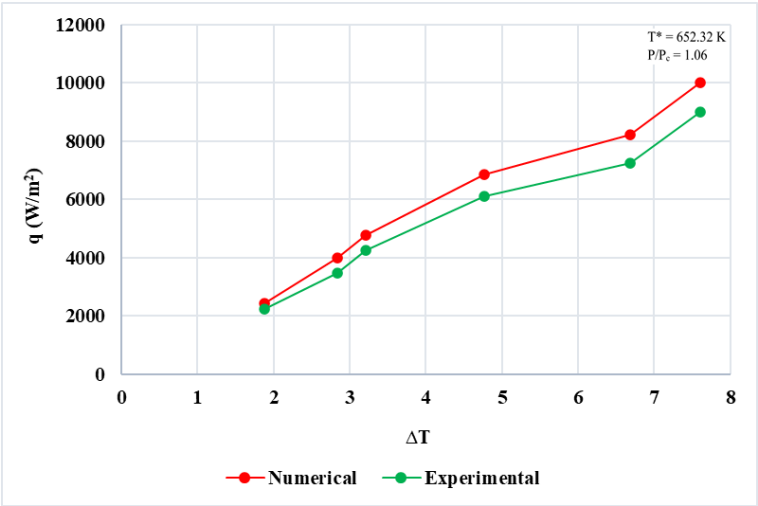

Fig. 10. Variation of *q* with *ΔT* for average T_∞= 652.20 K at *x* = 0.3 mfor 234.5 Bar

2.5 Boundary Conditions

The inlet free stream temperature is 643.16 K (T_∞) for all the simulations. Inlet free stream velocity varies for free and mixed convection. For free convection $u_\infty = 10^{-5}$ m/s $\left(\frac{Gr}{Re^2} > 10\right)$, and for mixed convection u_∞ = 0.070 m/s $\left(\frac{Gr}{Re^2} \text{ lies between } 0.1 \text{ and } 10\right)$.

2.6 Wall Temperature Variation

Wall temperature is a function of distance measured parallel to the direction of motion of fluid (*x*).

(a) Linear variation of wall temperature

The general form of linear variation of wall temperature can be written as

$$\frac{\Delta T(x)}{\Delta T_L} = ax + b \quad (1)$$

where $\Delta T(x) = T_w(x) - T_\infty$

If we assume that $\Delta T(x) = 0$ at x = 0, and if $\Delta T(x) = \Delta T_L$ at x= L, then Eq. (1) reduces to a simple form as

$$\frac{\mathbf{\Delta T(x)}}{\mathbf{\Delta T_L}} = \frac{\mathbf{x}}{\mathbf{L}}$$

Or,

$$\Delta T(x) = T_w(x) - T_\infty = \Delta T_L \left(\frac{x}{L}\right) \quad (2)$$

(b) Parabolic variation of wall temperature:

The parabolic variation of wall temperature with $\Delta T(x) = 0$ at x =0 gives the wall temperature distribution as,

$$\Delta T(x) = T_w(x) - T_\infty = \Delta T_L \left(\frac{x}{L}\right)^2 \quad (3)$$

Expressions for wall temperature as a function of distance from the leading edge Eq. (2) and Eq. (3) are incorporated as the wall temperature boundary conditions in numerical simulations.

3. Results and Discussion

3.1 Results for Free Convection

3.1.1 Velocity and temperature profiles for linear wall temperature variation case

Figure 11 and Figure 12 show the velocity profiles for linear wall temperature variation, for water at 225 bar and 235 bar and at x = 0.06 m, for five different values of ΔT_L It can be seen from these figures that, the maximum velocity in the boundary layer increases with increase in ΔT_L and the location at which this maximum occurs shifts towards the wall.

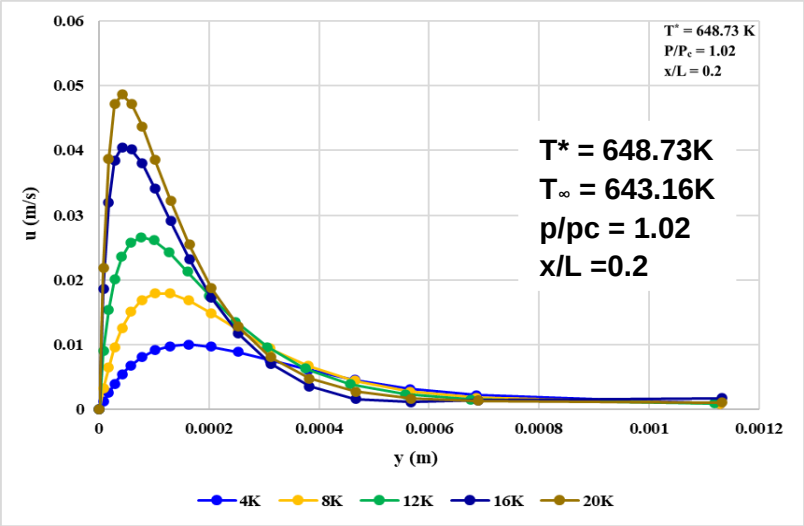

Fig. 11. Velocity profiles for different values of ΔT_L at x = 0.06 m for water at 225 bars for free convection with linear wall temperature variation

Similar profiles are obtained for the case of parabolic variation of wall temperature also (not shown), except that for linear variation of wall temperature, the maximum velocity in the boundary layer increases from 0.015 for ΔT_L = 4 K to 0.052 m/s for ΔT_L = 20 K , while for parabolic variation of wall temperature, the corresponding maximum velocity decreases to 0.01 m/s for ΔT_L = 4 K to 0.049 m/s for ΔT_L = 20 K .This is obvious because, for the same value of ΔT_L and for same x, parabolic wall temperature variation gives lower value of T_w than that for linear variation of wall temperature at any x between 0 and L , thereby reducing the buoyancy force and hence the velocity.

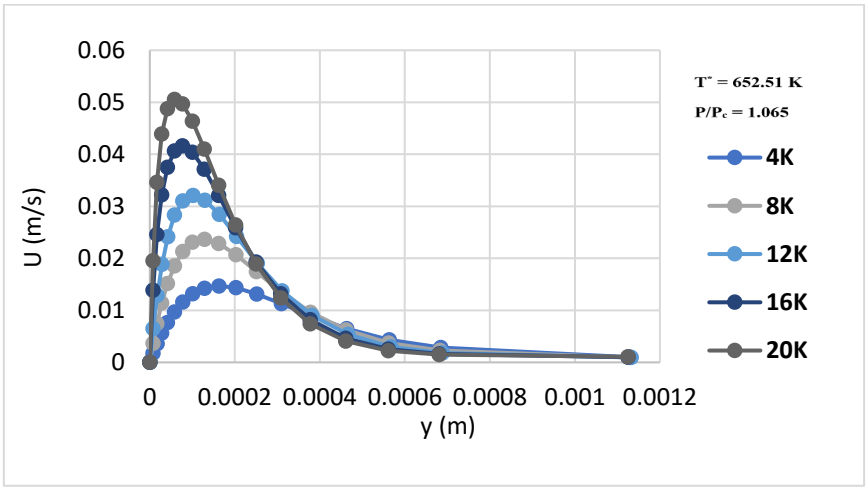

Fig. 12. Velocity profiles for different values of ΔT_L at x = 0.06 m for water at 235 bars for linear wall temperature variation

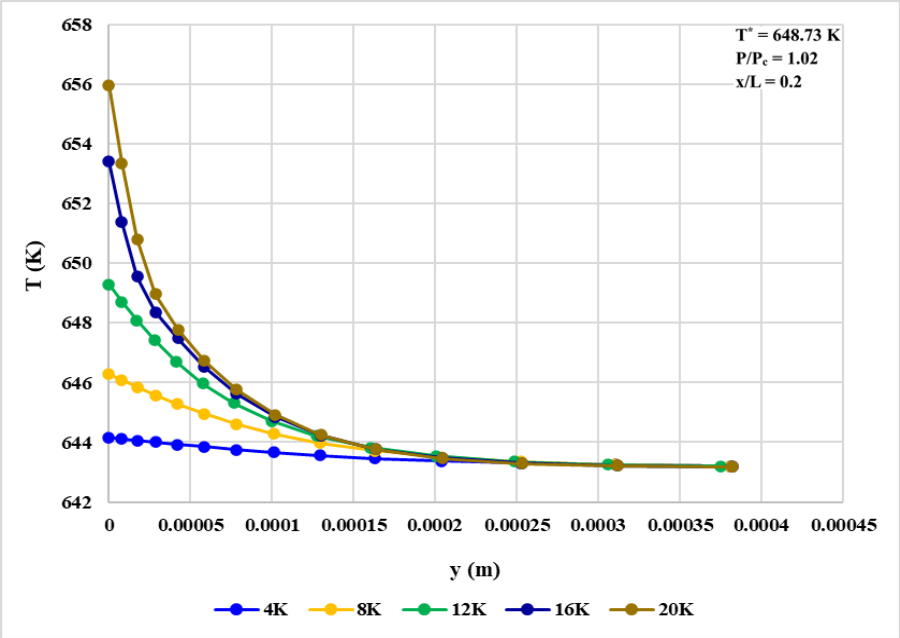

Fig. 13. Temperature profiles for different values of ΔT_L at x = 0.06 m for water at 225 bars for linear wall temperature variation

The temperature profiles for different values of ΔT_L ($\Delta T_L = [T_w]_{x=L} - T_\infty$) for water at 225 bar and 235 bar respectively for x = 0.06 m for linear wall temperature variation are shown in Figure 13 and Figure 14. It can be seen from these figures that as ΔT_L increases the temperature gradient at the wall increases and hence increases the wall heat flux, resulting in higher heat transfer coefficients. Further, the temperature gradient at the wall for all values of ΔT_L is higher for 225 bar than that for 235 bar pressure resulting in higher wall heat flux, and hence higher heat transfer coefficient. Similar profiles are obtained for parabolic variation of wall temperature also.

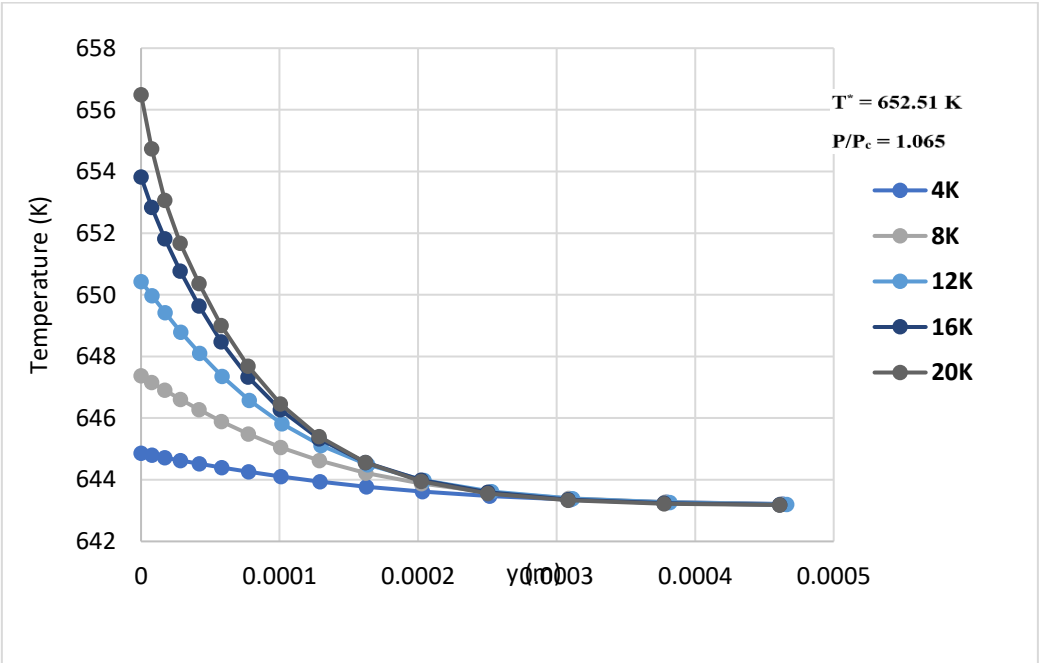

Fig. 14. Temperature profiles for different values of ΔT_L at x = 0.06 m for water at 235 bars for linear wall temperature variation

3.1.2 Wall heat flux and heat transfer coefficient for linear wall temperature case

The variation of wall heat flux with x for different values of ΔT_L for free convection for linear wall temperature variation are shown in Figure 15 and Figure 16 respectively. It can be seen from Figure 15 that, for values of ΔT_L equal to 4 K and 8 K, the wall heat flux increases with x for the entire length considered. But for the remaining values of ΔT_L, the wall heat flux increases with x up to a certain length and then remains practically constant over a certain length and then once again increases with x. This effect will persist up to a certain length. This nature of variation can be attributed to the fact that for all these cases T* lies in the boundary layer. For the case of ΔT_L= 12 K, $T_w \approx T^*$ for x equal to about 0.008m and one can expect the distortion of the velocity and temperature profiles for this value of x and this distortion will result in decreasing the temperature gradient and hence the wall heat flux. This effect will persist up to certain value of x, with the result, there is hardly any variation of wall heat flux with x. Beyond this value of x, the location of T* will be considerably away from the wall and presence of T* will not affect the temperature gradient at the wall and hence the wall heat flux.

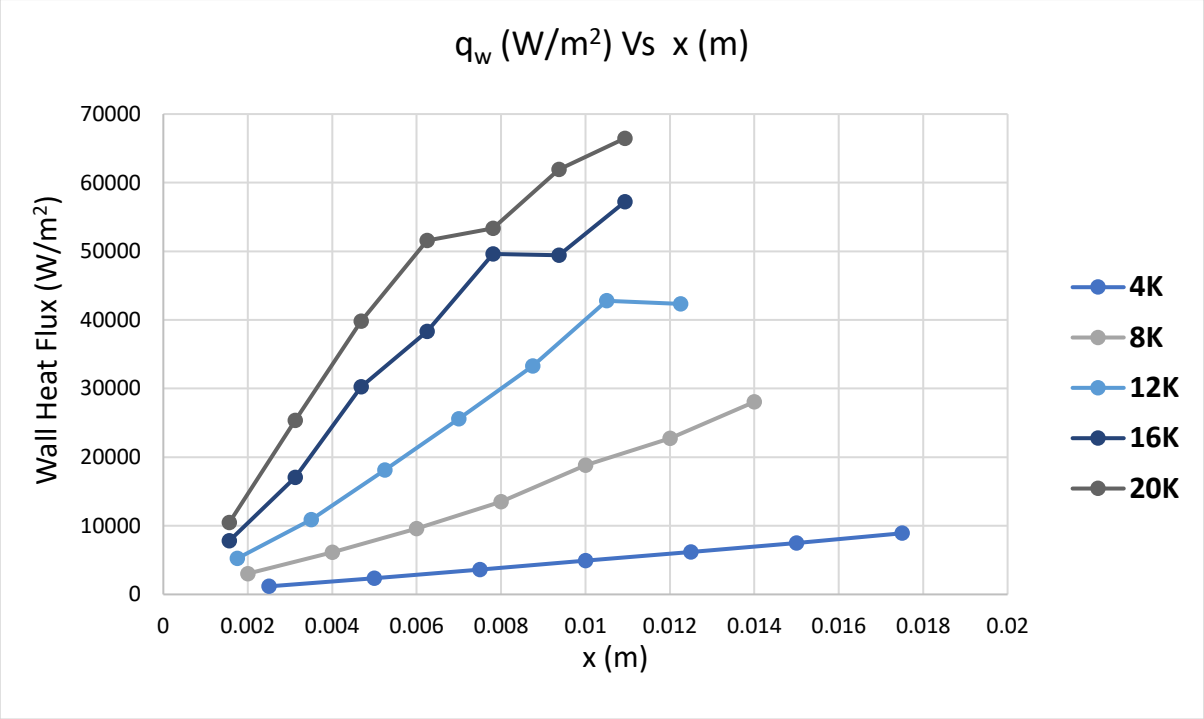

Fig. 15. Variation of wall heat flux with x for free convection for different values of ΔT_L for water at 225 bars for linear wall temperature variation

Similar nature of variation of will heat flux with x is predicted for 235 bar also as shown in Figure 16, except that the effect of T* is not so significant as for the case for 225 bar pressure.

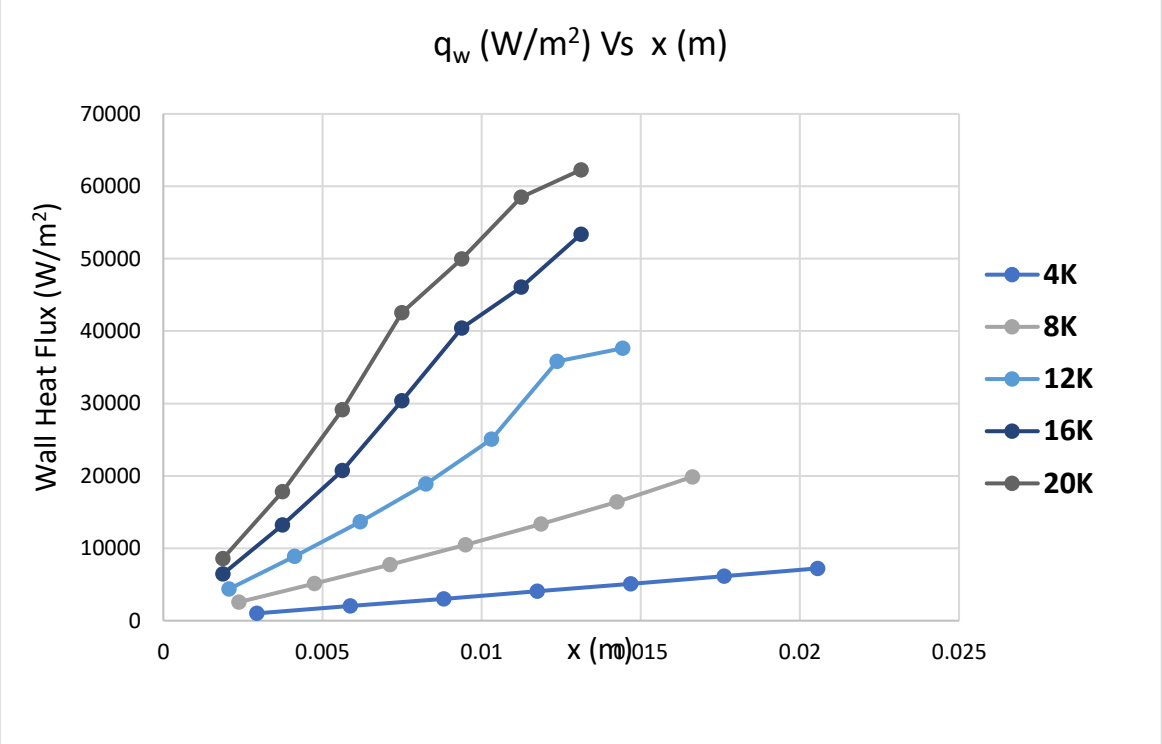

Fig. 16. Variation of wall heat flux with x for different values of ΔT_L for free convection for water at 235 bars for linear wall temperature variation

In order to know the influence of the nature of wall temperature distribution on the wall heat flux, a plot of wall heat flux versus x for two different values of ΔT_L, namely, ΔT_L = 4 K, for which T* does not lie within the boundary layer, and ΔT_L = 16 K for which T* lies within the boundary layer, is shown in Figure 17 for 225 bar pressure for both linear wall temperature and parabolic variation of wall temperature. It can be seen from this figure, that for the case of ΔT_L = 4 K, T* does not lie within the boundary layer, the wall heat flux is higher for the linear wall temperature for all values of x, though the difference in magnitude is not very significant. On the other hand, for ΔT_L = 16 K, where T* lies within the boundary layer, the plot shows that the wall heat flux for linear wall temperature case is significantly different from that for the parabolic wall temperature case till a value of x (say x*) is reached. At x = x*, for the liner wall temperature case there is a sudden change in the slope, such that (dq_w/dx) is practically zero and this persists up to a certain value of x, beyond which q_w increases with x. But this type of variation is not observed for the parabolic wall temperature case and further the rate of increase of q_w is quite large for parabolic wall temperature case.

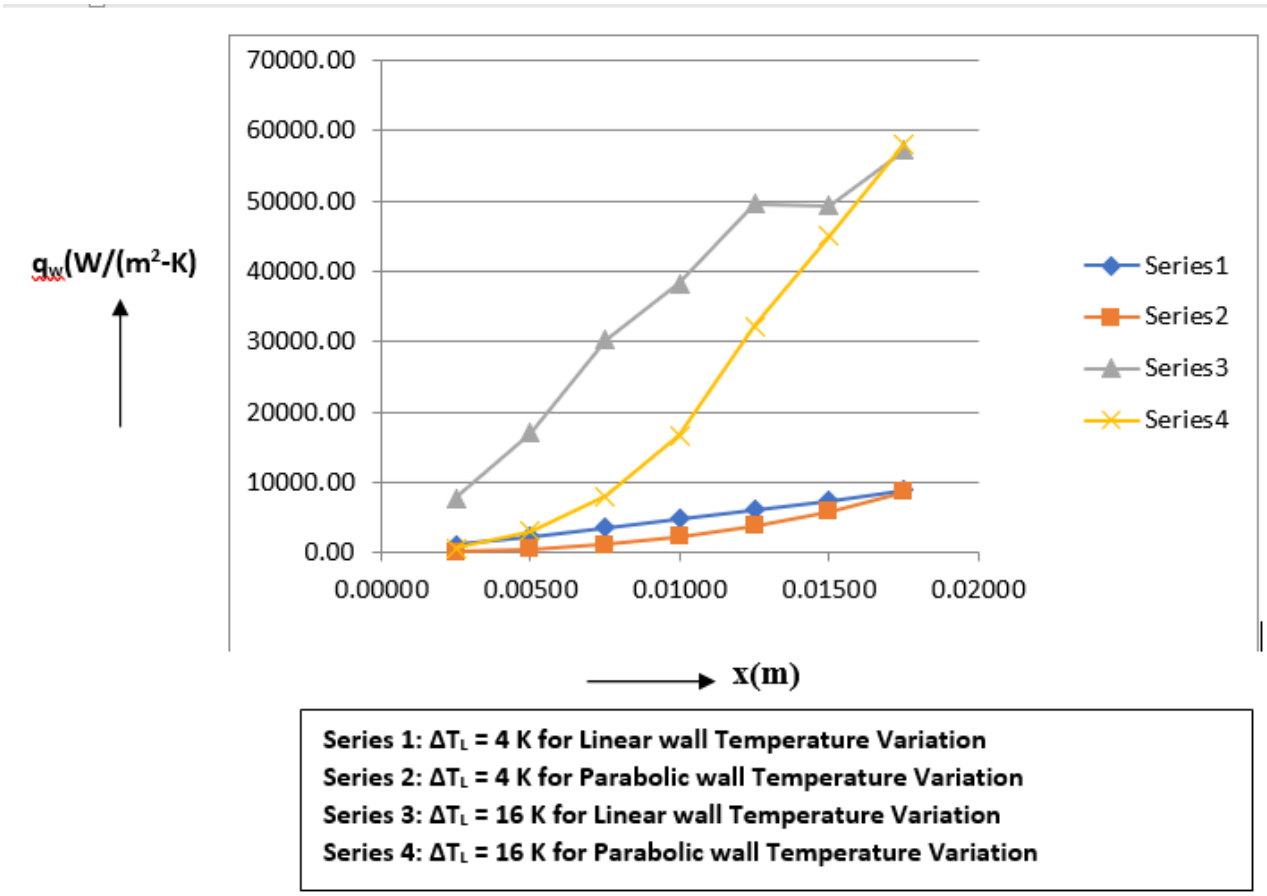

Fig. 17. Variation of wall heat flux with x for two values of ΔT_L for free convection for water at 225 bars for both linear and parabolic wall temperature variations

Figure 18 and Figure 19 show the variation of heat transfer coefficient, h with x for five different values of ΔT_L at x = 0.06 m for water at 225 bar and 235 bar respectively, for linear wall temperature variation. It can be seen from Figure 18, that, for ΔT_L = 4 K and 8 K, h increases with x continuously, where as for other values of ΔT_L, h initially increases with x, reaches a maximum and then decreases with increase in x. This due to the effect of T* on the temperature profile. It can also be seen from Figure 18, that the value of x at which the maximum heat transfer coefficient occurs decreases with increase in ΔT_L.

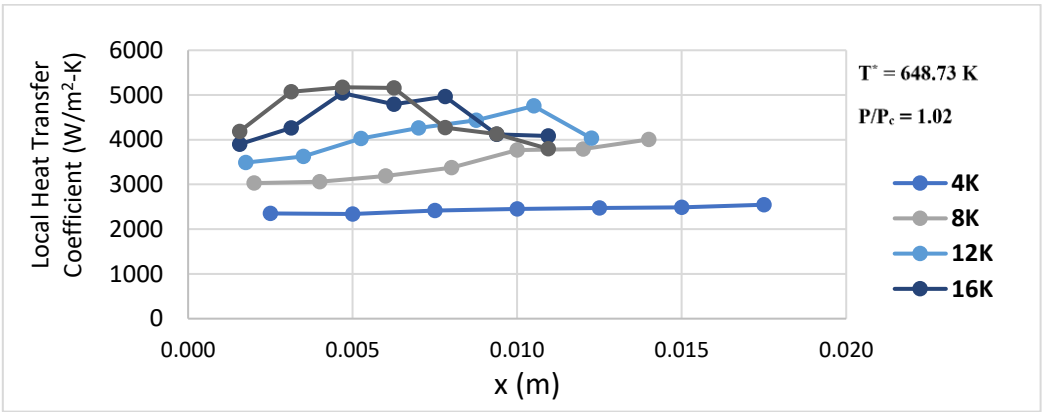

Fig. 18. Variation of h with x for different values of ΔT_L for free convection for water at 225 bars with linear wall temperature variation

The plot for 235 bar shown in Figure 19, indicates a similar behavior of h with respect to x, but the variation is smoother than that for 225 bar pressure. It can also be seen from this figure that for 235 bar pressure, for ΔT_L = 4 K (for this case T* does not within the boundary layer), h remains practically constant, whereas for the remaining cases, the rate of increase of h with x is significantly lower than that for 225 bar pressure.

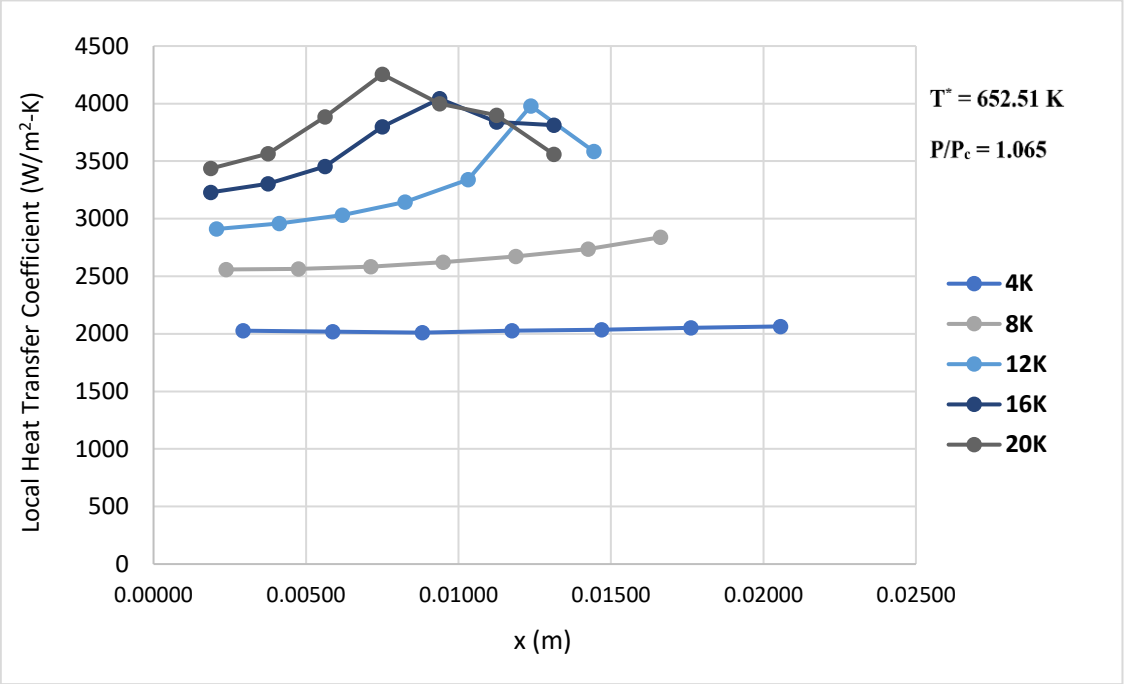

Fig. 19. Variation of h with x for different values of ΔT_L for water at 235 bars for free convection with linear wall temperature variation

Figure 20 shows the variation of heat transfer coefficient with x for both linear and parabolic variation of wall temperature cases two different values of ΔT_L and for 225 bars. This plot is shown to know the influence of the nature of wall temperature variation on the heat transfer coefficient. It can be seen from this figure, for ΔT_L = 4 K, where T* does not lie within the boundary layer, h remains practically constant for linear wall temperature case, whereas for the parabolic wall temperature variation, h remains constant up to a certain value of x and then increases with increase in x.

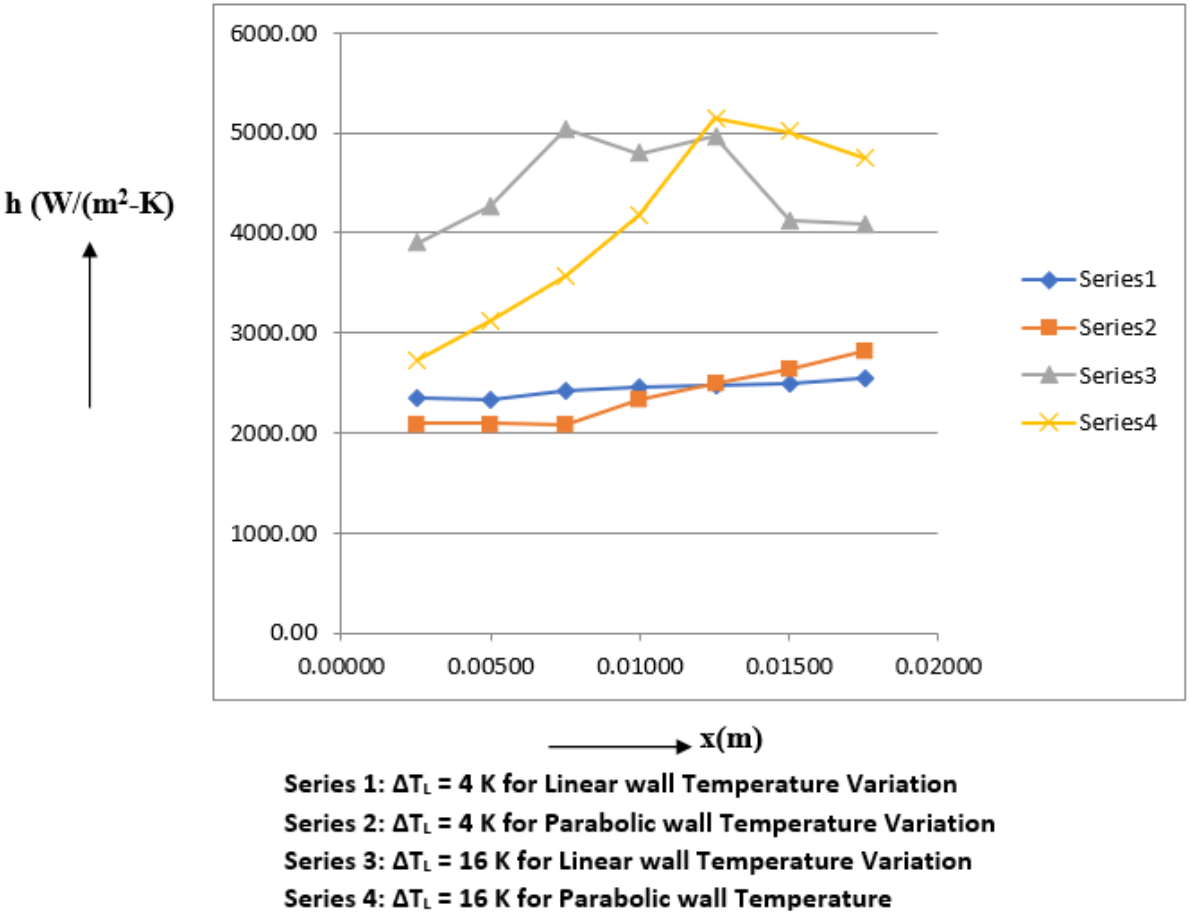

Fig. 20. Variation of h with x for two values of ΔT_L for water at 225 bars for free convection for both linear and parabolic wall temperature variations

Also, the heat transfer coefficient will be higher for the linear wall temperature case up to a certain value of x and then h will be higher for the parabolic wall temperature case. For ΔT_L = 16 K when T* lies within the boundary layer, the heat transfer initially increases with x, reaches a maximum and then decreases with increase in x. for both linear wall temperature and parabolic wall temperature cases. The location of maximum value of h occurs at a value of x at which $T_w \approx T^*$. The maximum value of h occurs at lower value of x for the linear wall temperature case. Further it should be noted that, up to a certain value of x, the linear wall temperature case gives higher value of h than that for the parabolic wall temperature case. Beyond this value of x, the parabolic wall temperature gives higher value of h than that for the linear wall temperature case.

3.1.3 Nusselt number for linear wall temperature case

Figure 21 and Figure 22 shows the variation of local Nusselt number with x/L for five different values of ΔT_L for water at 225 bar and 235 bar pressure respectively for linear wall temperature variation. It can be seen from Figure 17, that for ΔT_L = 4 K ($\Delta T_L < \Delta T^*$), Nu_x increases almost linearly with x. For cases When ΔT_L= 8, 12, 16 and 20 K, $\Delta T_L > \Delta T^*$, T^* lies within the boundary layer and hence the variation of Nu_x will be different from the case when ΔT_L = 4 K. For these cases, Nu_x increases with x up to around x^* (x^* is the value of x at which $T_w = T^*$) and then remain practically constant up to a wall temperature several degrees higher than T^* and then once again increases with increase in x. Similar variation is predicted for 235 bar pressure, except that for all the values of ΔT_L, there is no

sudden change in the rate of change of Nu_x with x, but the change is more gradual. This is because at 235 bar pressure the c_p with respect to T is not so severe as for the case when the pressure is 225 bar.

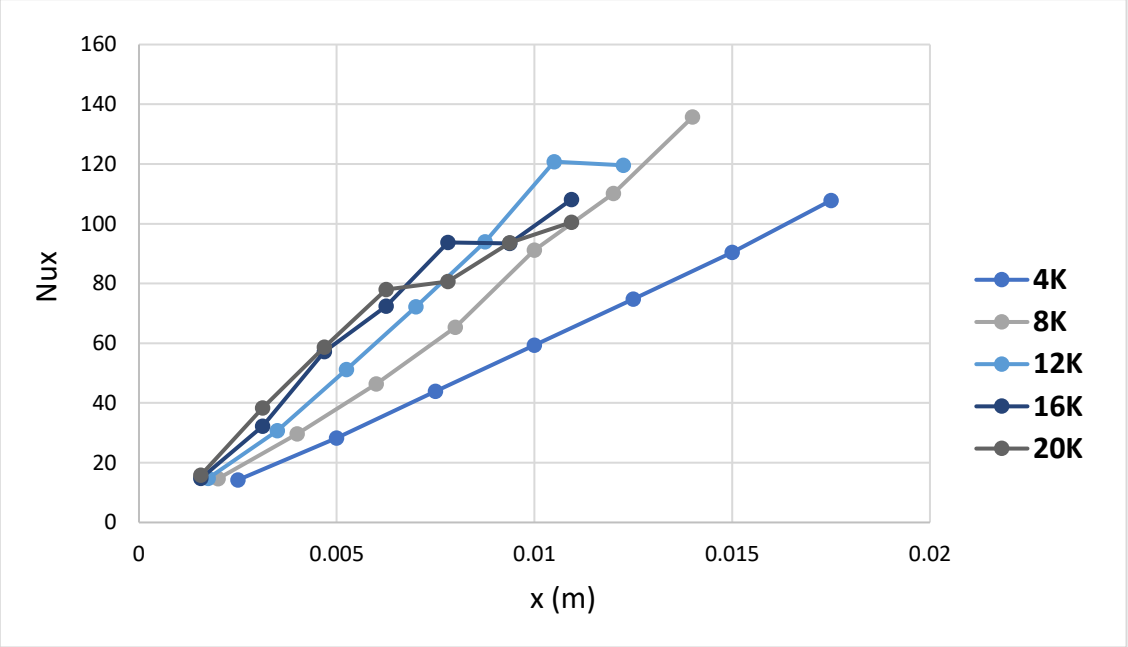

Fig. 21. Variation of Nussekt number with x for five different values of ΔT_L for water at 225 bar for free convection with linear wall temperature variation

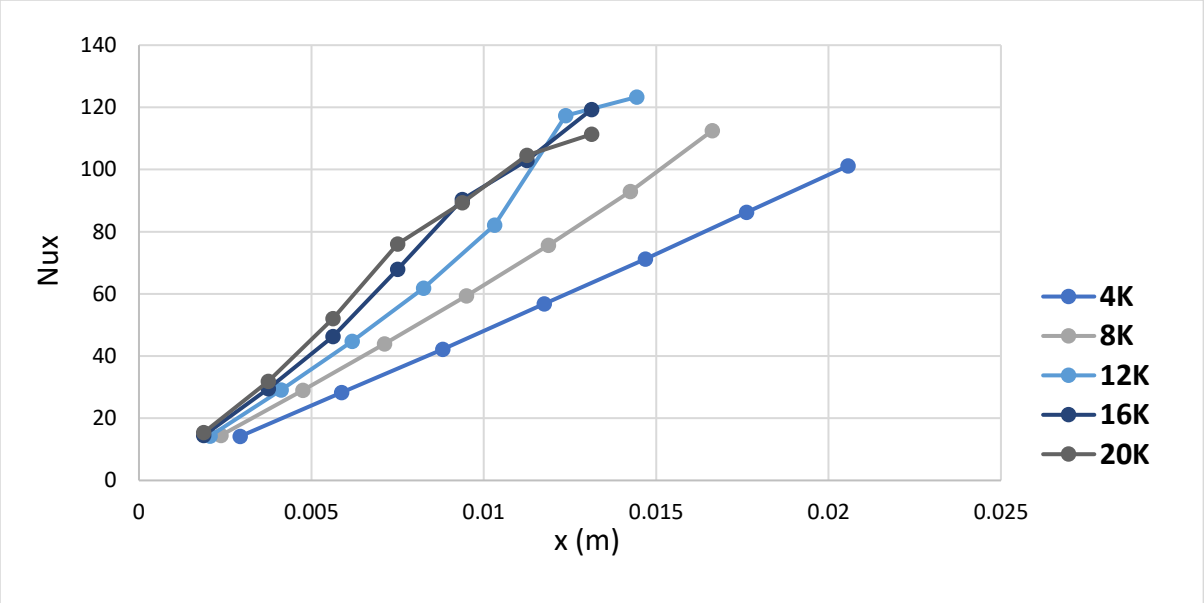

Fig. 22. Variation of Nussekt number with x for five different values of ΔT_L for water at 225 bars for free convection with linear wall temperature variation

Figure 23 shows the variation of Nusselt number with x for both linear and parabolic variation of wall temperature variations for two different values of ΔT_L and for 225 bars. This plot is shown to know the influence of the nature of wall temperature variation on the Nusselt number. It can be seen from this figure for ΔT_L equal to 4 K, where T* does not lie within the boundary layer for both the linear wall temperature case and the parabolic wall temperature case, Nu_x increases continuously with x, the variation being quite smooth. Also, the difference in Nu_x between the linear wall

temperature case and the parabolic wall temperature case is not very significant. For the linear wall temperature case, Nu_x varies linearly with x, whereas, for the parabolic wall temperature case the variation is nonlinear resulting in higher values of Nu_x for large values of x in comparison with linear wall temperature case. For the case when ΔT_L = 16 K, T* lies within the boundary layer and this has significant influence on the variation of Nu_x with x. For the linear wall temperature case, Nu_x, increases initially with x up to a certain value and then remains practically constant and finally increases with x. But for the parabolic wall temperature case, the variation of Nu_x is smooth but there is a change of slope at x ≈ 0.0125 m.

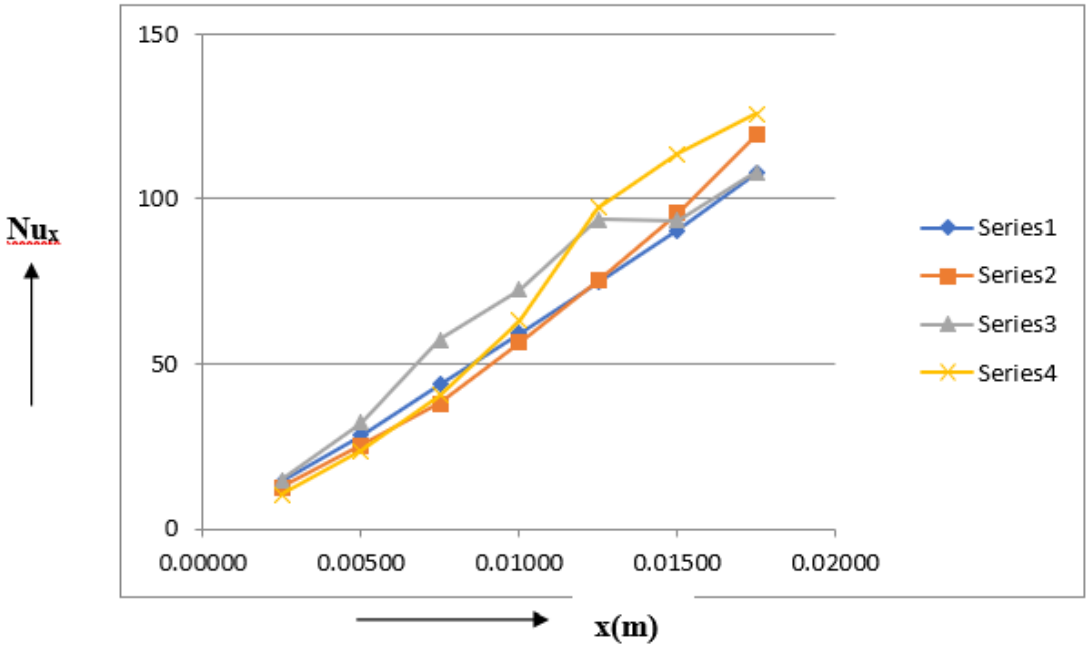

Series 1: ΔT_L = 4 K for Linear wall Temperature Variation
Series 2: ΔT_L = 4 K for Parabolic wall Temperature Variation
Series 3: ΔT_L = 16 K for Linear wall Temperature Variation
Series 4: ΔT_L = 16 K for Parabolic wall Temperature Variation

Fig. 23. Variation of Nussekt number with x for two different values of ΔT_L for water at 225 bars for free convection with linear wall temperature and parabolic wall temperature variations

3.1.4 Correlations for free convection for linear wall temperature case and for parabolic wall temperature case

Two correlations to evaluate the Nusselt numbers are proposed based on numerical predictions, using multiple regression analysis. One correlation is for the case of linear wall temperature variation and the other for parabolic variation of wall temperature. The form of correlation is based on the recommendations of Ghorbani aand Gajjar [23] who have recommended that all the propertry ratios, namely,ρ^*,μ^*,k^* and c_p^* shuld be taken into account in the correlation.

Using multiple regression analysis and using 70 data points, the correlation for free convection from vertical flat plate with linear wall temperature is given by with maximum deviation being ± 10 percent.and R^2 value of 0.997.

$$(Nu_{fl})_c = 0.563(Ra_x)^{0.253}(\rho^*)^{-0.56}\left(c_p^*\right)^{0.423}(\mu^*)^{0.099}(k^*)^{0.095} \quad (4)$$

Figure 24 shows the deviation of all the data points from correlation curve for linear wall temperature variation.

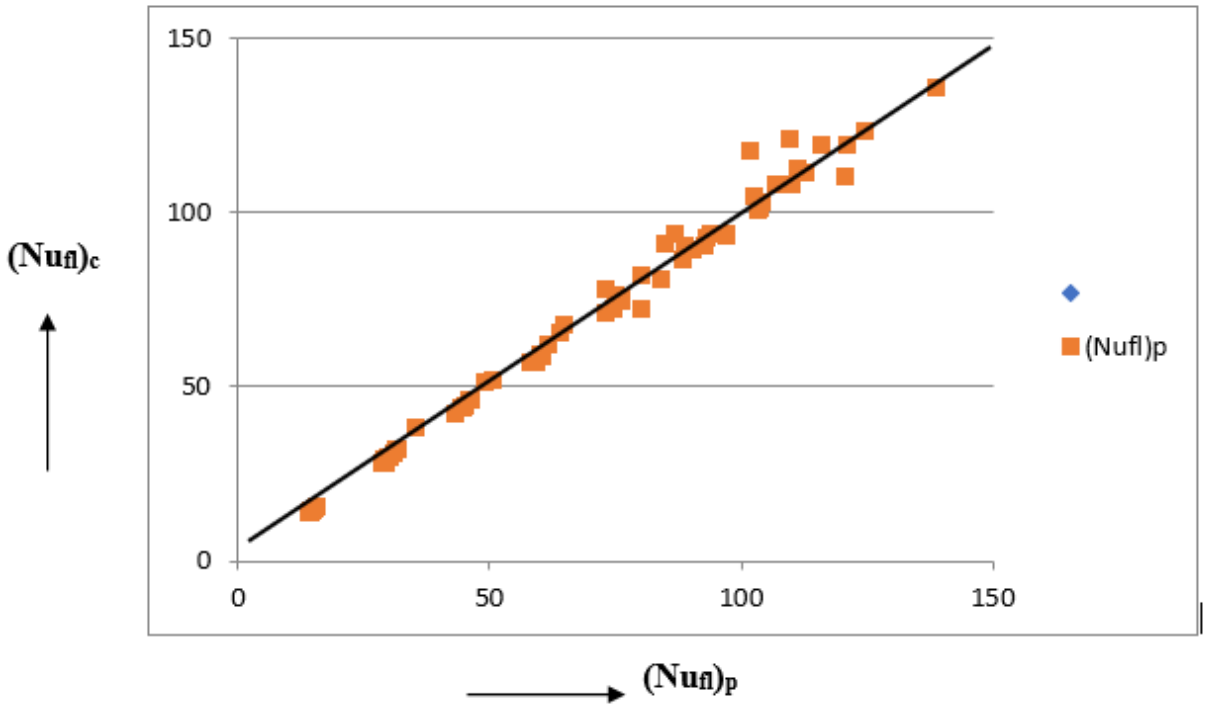

Fig. 24. Comparison between Nusselt number calculated using Eq.(4), $(Nu_{fl})_c$ and predicted Nusselt number, $(Nu_{fl})_p$

The correlation for Nusselt number for the parabolic variation of wall temperature is given by

$$(Nu_{fp})_c = 0.849\ (Ra_x)^{0.223}(\rho^*)^{-0.56}\left(c_p^*\right)^{0.214}(\mu^*)^{1.417}(k^*)^{-0.07} \quad (5)$$

with maximum deviation being ± 11 percent. Except for two data points for which the deviation is ± 15 percent and R^2 value is 0.996. The comparison between the Nusselt number calculated using Eq. (5) and the one predicted is shown in Figure 25.

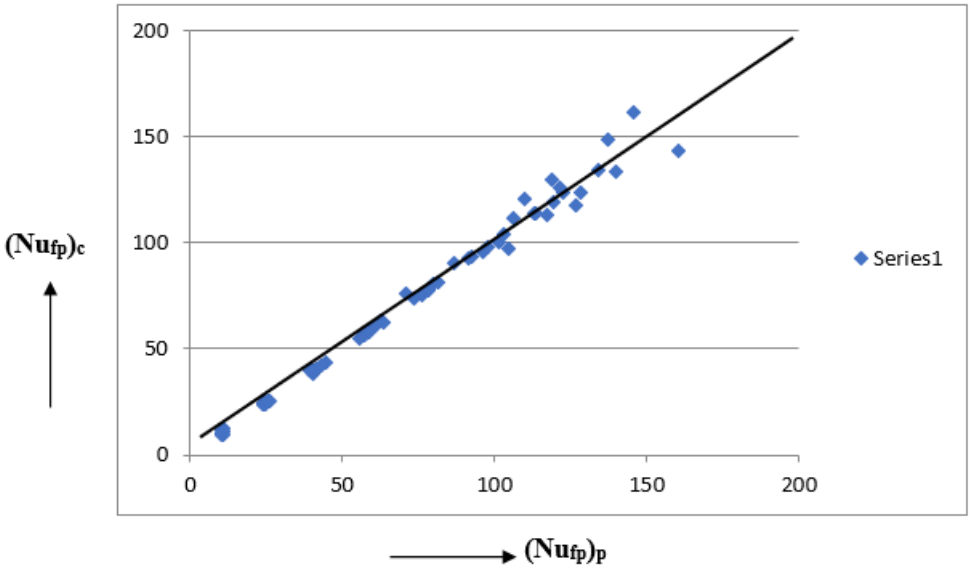

Fig. 25. Comparison between Nusselt number calculated using Eq.(5), $(Nu_{fp})_c$ and predicted Nusselt number, $(Nu_{fp})_p$ for free convection

3.2 Results for Mixed Convection

3.2.1 Velocity and temperature profiles for parabolic variation of wall temperature

The velocity profiles for five different values of ΔT_L and for 235 bar pressure and at x = 0.06 m, is shown in Figure 26 for parabolic variation of wall temperature. It can be seen from this figure that for the case of ΔT_L = 4 K, the velocity profile is smooth without any distortion. It should be noted that for this case T* does not lie within the boundary layer. For other cases, there is distortion of the velocity profile as, T* lies within the boundary layer. The amount of distortion and the value of y at which this distortion occurs depends on how close this location is to the wall. For ΔT_L = 20 K, this location is very close to the wall, where as for other values of ΔT_L the distortion occurs at a much higher value of y. The distortion in the profile will influence the velocity and temperature gradients at the wall, which in turn influence the drag coefficient and the heat transfer coefficient. Similar nature of variation is predicted for linear wall temperature variation also.

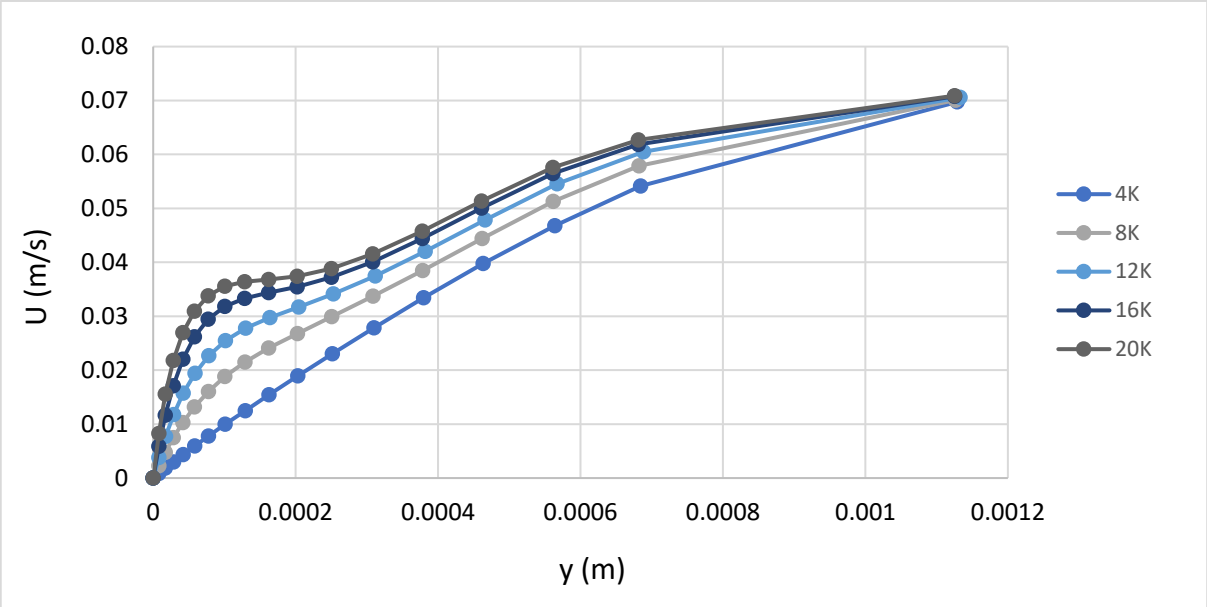

Fig. 26. Velocity profiles for different values of ΔT_L and for 235 bar at x = 0.06 m for parabolic variation of wall temperature

Figure 27 shows the temperature profile for five different values of ΔT_L and for 235 bar pressure at x = 0.06 m for parabolic variation of wall temperature. It can be seen from Figure 27 that,the temperature gradient at the wall increses as ΔT_L increases,indicating that higher the value of ΔT_Lwill give higher wall heat flux.Also the rate of change of T with respect to y,$\left(\frac{dT}{dy}\right)$ at any y increases with increase in ΔT_L. Similar nature of variation is predicted for linear wall temperature case also.

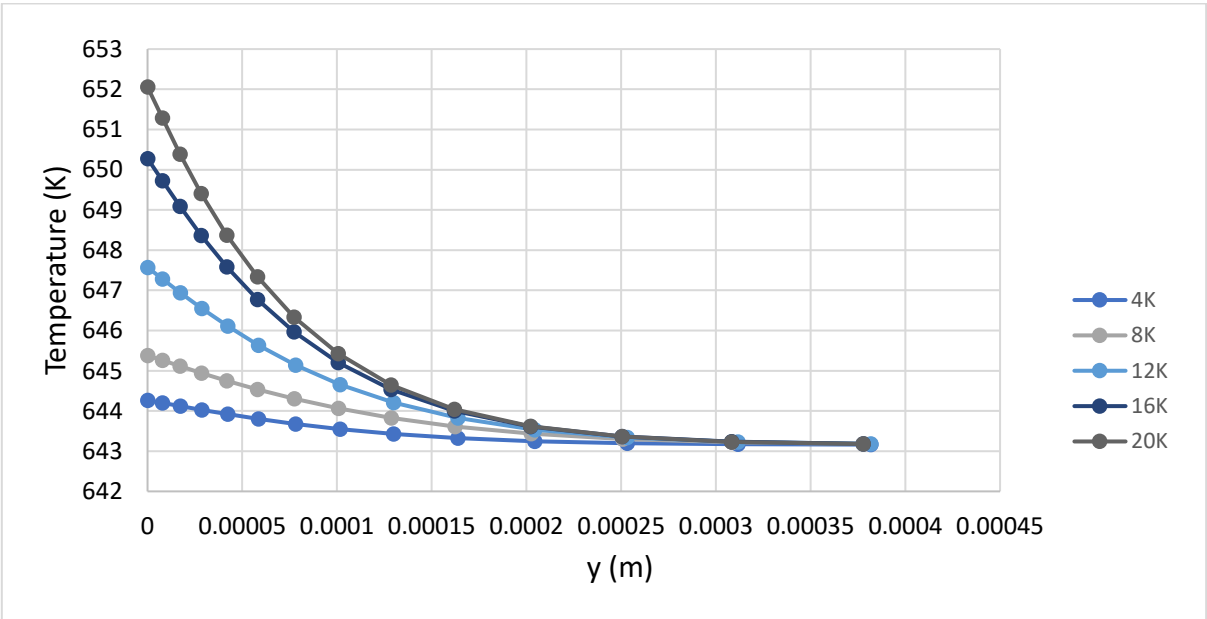

Fig. 27. Temperature profiles for different values of ΔT_L and for 235 bar at x = 0.06 m for parabolic variation of wall temperature

3.2.2 Wall heat flux and heat transfer coefficient for mixed convection with parabolic wall temperature variation

The variation of wall heat flux with x for five different values of ΔT_L is shown in Figure 28 and Figure 29 for 225 bar and 235 bar pressures respectively, for parabolic variation of wall temperature. Figure 28 indicates that for all cases except for thae case, ΔT_L = 20 K, wall heat flux increases with x smoothly, where as for the case of ΔT_L = 20 K, wall heat flux increases smoothly with x up to about x = 0.009 m, beyond which the rate of increse of wall heat flux decreses with increases in x. This sudden change in the slope $\left(\frac{dq_w}{dx}\right)$ at x ≈ 0.008 may be attributed to the fact that at this value of x, T* is closer to the wall to influence the temperature gradient at the wall and hence the wall heat flux.

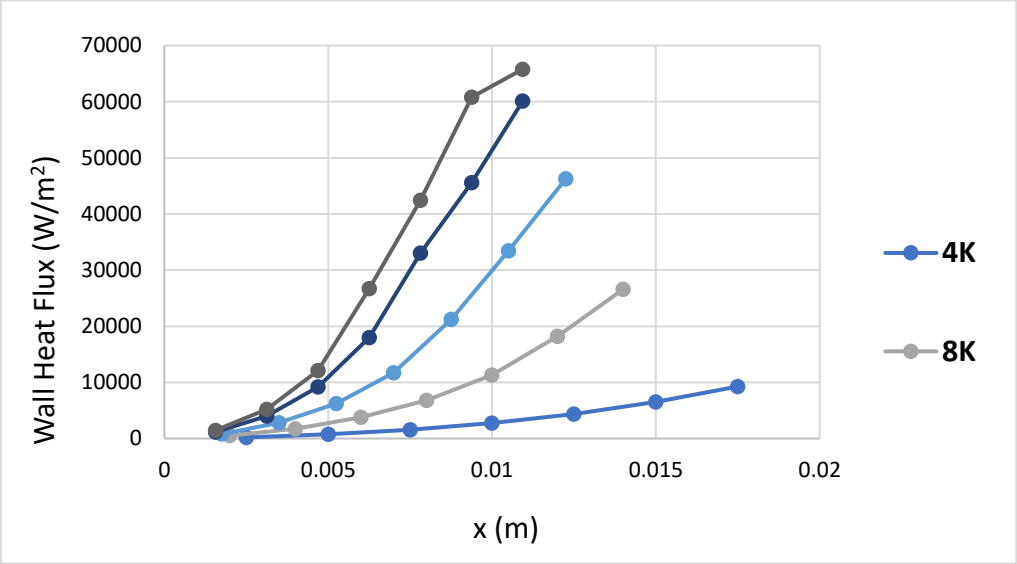

Fig. 28. Variation of wall heat flux with x for five different values of of ΔT_L for water at 225 bars for mixed convection with parabolic wall temperature variation

For 235 bar pressure (Figure 29), the nature of variation of wall heat flux with x is similar to the case of 225 bar pressure, except that, for 225 bar pressure ,it is higher than that for 235 bar pressure and this is true for all values of ΔT_L.

In order to know the influence of the nature of wall temperature distribution on wall heat flux, plot of wall heat flux with respect to x is shown in Figure 30 for two values of ΔT_L., namely, ΔT_L = 4 K for which T* does not lie within the boundary layer, and ΔT_L = 16 K for which T* lie within the boundary layer .It can be seen from this plot that the wall heat flux for linear wall temperature case is higher than the parabolic wall temperature case , though the difference is insignificant for ΔT_L = 4 K for which T* does not lie within the boundary layer. However, for ΔT_L = 16 K, T* lies within the boundary layer and its effect on the temperature profile and hence the wall heat flux can be seen for the linear wall temperature case at x ≈ 0.0125.m. From this value of x onwards, the wall heat flux remains practically constant up to a certain value of x and then q_w increases with increase in x. This trend is observed for free convection case also. As far as the parabolic wall temperature case is concerned, abrupt change in the value of (dq_w/dT) is not predicted for values of x up to about 0.0175 m.

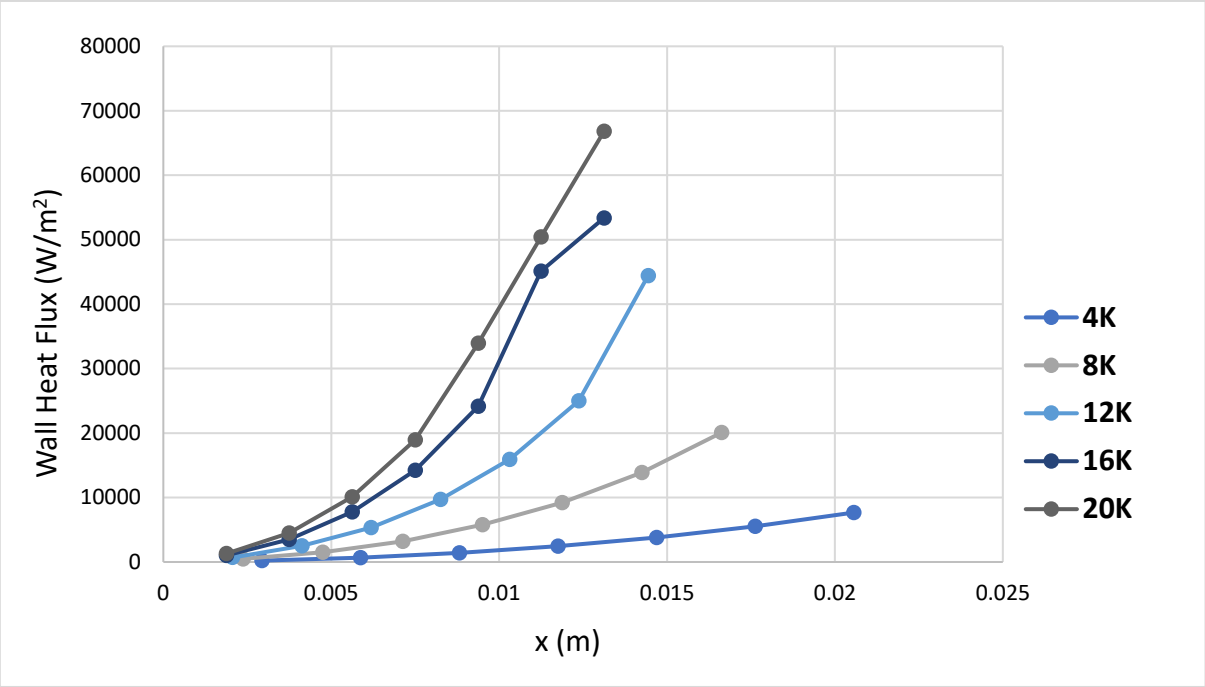

Fig. 29. Variation of wall heat flux with x for five different values of of ΔT_L for water at 235 bars for mixed convection with parabolic wall temperature variation at any x, (dqw/dx)

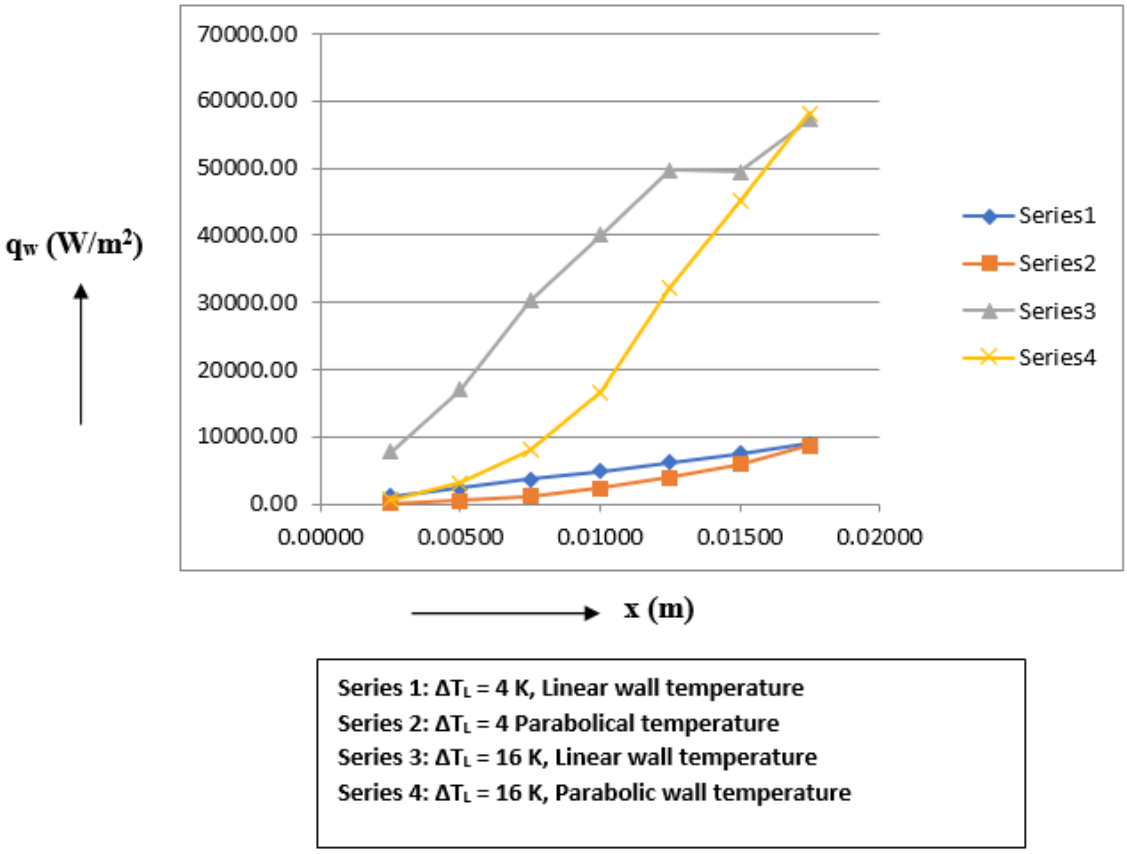

Fig. 30. Variation of wall heat flux with x for two values of ΔT_L for 225 bar pressure for linear wall temperature and parabolic wall temperature cases

The variation of the heat transfer coefficient with x is shown in Figure 31 and Figure 32 for five different values of ΔT_L for 225 bar and 235 bar pressures respectively, for parabolic variation of wall temperature. It can be seen from Figure 30, that for 225 bar pressure, for ΔT_L equal to 4 K (for this case, T* does not lie within the boundary layer), h decreses with x, reaches a minimum and then gradually increases with respect to x. However for 235 bar pressue for the same value of ΔT_L = 4 K, the nature of variation is similar to that for 225 bar pressure, but the rate of change of h with x is higher. This is true for ΔT_L equal to 8 K and 12 K for both the pressures. However, for ΔT_L equal to 16 K and 20 K, the nature of variation of h with x is quite different, but similar for the two pressures. For these two values of ΔT_L, h decreases with increase in x, reaches a minimum and then increases with x, reaches maximum and then once again decreases with increase in x. This nature of variation of h with x can be attributed to the location of T* in the boundary layer with respect to the wall. Similar nature of variation is predicted for linear wall temperature case also.

The influence of the nature of wall temperature distribution on the heat transfer coefficient is illustrated in Figure 33. In this figure variation of h with x is plotted for two values of ΔT_L, namely ΔT_L = 4 K for which T* does not lie within the boundary layer, and ΔT_L = 16 K for which T* lies within the boundary layer. It can be seen from this plot for the case for which T* does not lie within the boundary layer, for the linear wall temperature case, h remains practically constant with respect to x, whereas for the parabolic wall temperature case, h remains constant, but less than h for the linear wall temperature case up to a certain value of x and then h increases with x and become higher than that for linear wall temperature case. For the case of ΔT_L = 16 K for which T* lies within the boundary layer, h for linear wall temperature case is higher than for the parabolic wall temperature case up to x ≈ 0.0125 m, beyond which, h for linear wall temperature case become less than that for the parabolic case. In addition, for the linear wall temperature case h is practically constant for certain range of x and then it decreases significantly with increase in x. The range of x in which h remain constant is the range in which the wall temperature is in the neighborhood of T* at which the property variations are very severe and this could be the cause for sudden change in the value of h.

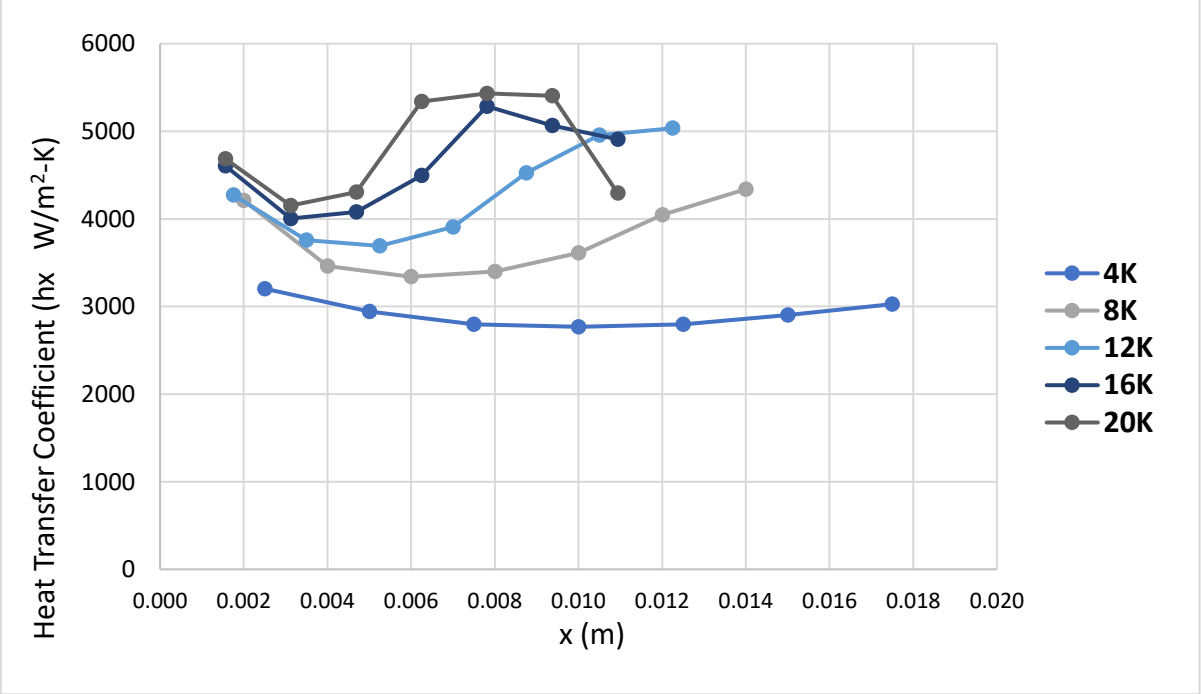

Fig. 31. Variation of h with x for five different values of ΔT_L for water at 225 bars for mixed convection with parabolic wall temperature variation

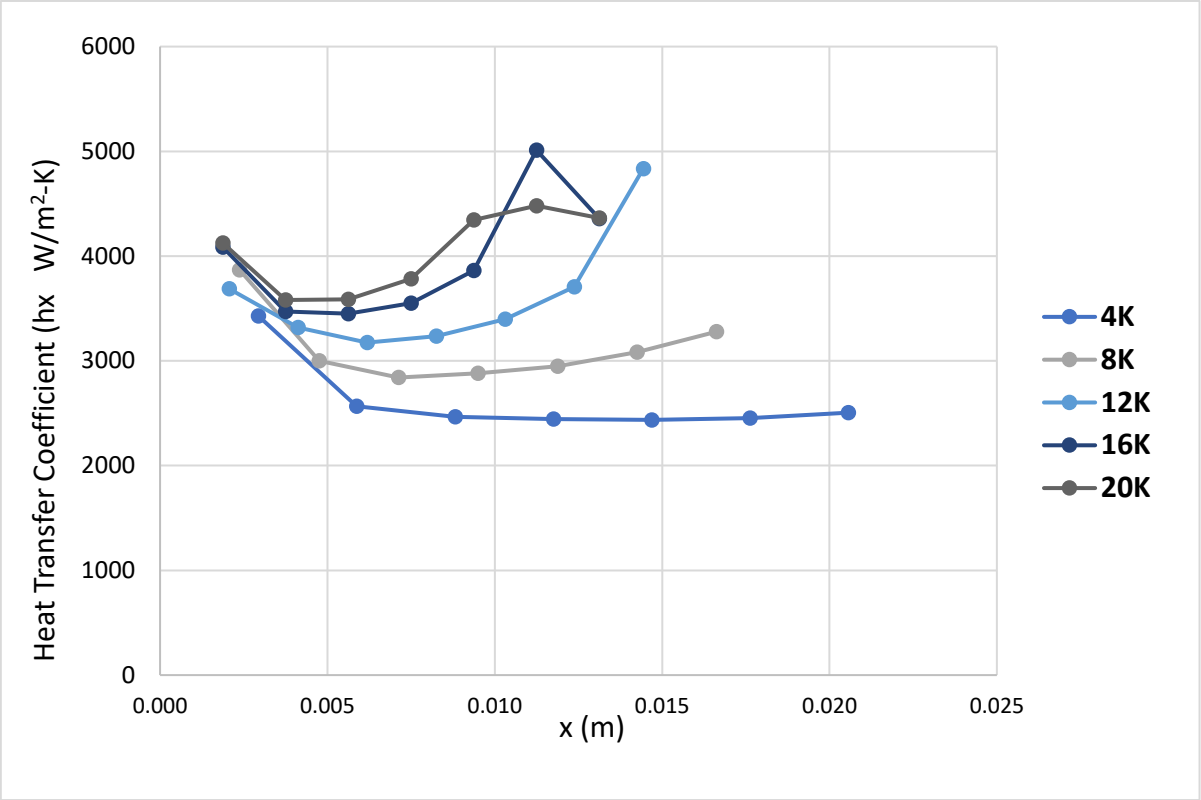

Fig. 32. Variation of h with x for five different values of ΔT_L for water at 235 bars for mixed convection with parabolic wall temperature variation

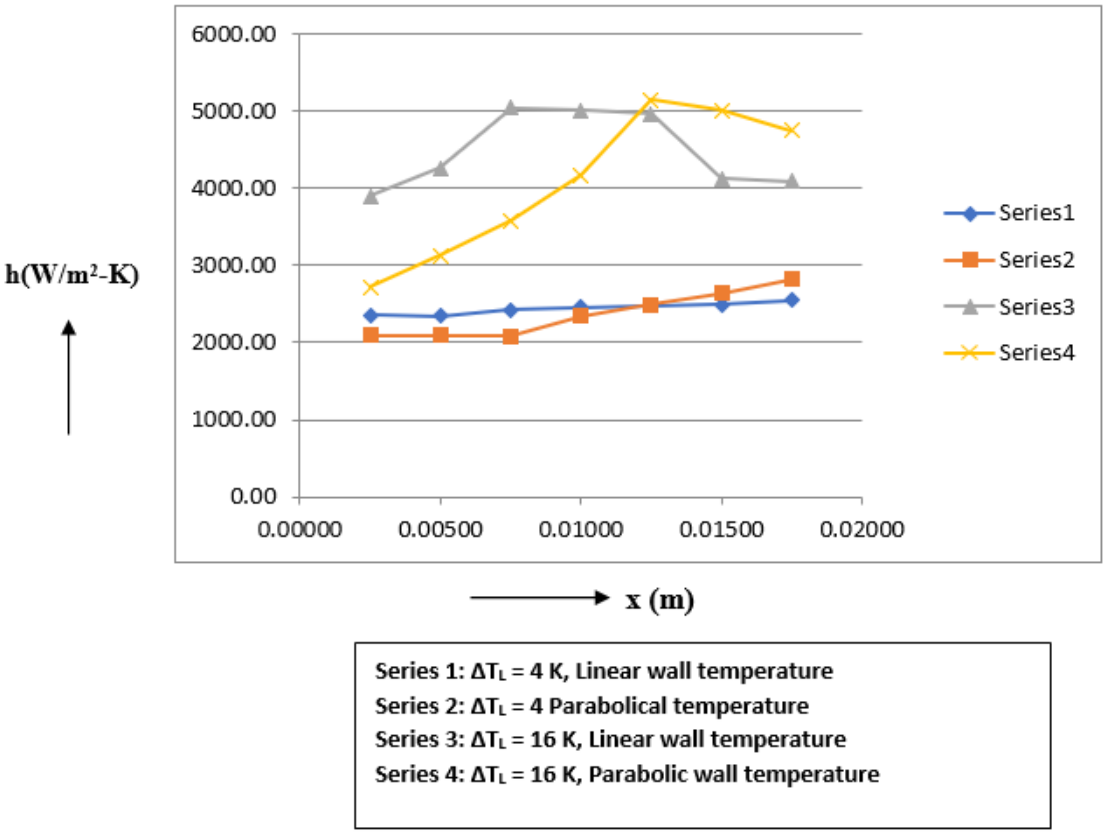

Fig. 33. Variation of h with x for two values of ΔT_L for 225 bar pressure for linear wall temperature and parabolic wall temperature cases

The variation of Nu with x is shown in Figure 34 for five different values of ΔT_L for water at 235 bars for mixed convection with parabolic variation of wall temperature. It can be seen from this figure that, except for ΔT_L = 20 K Nu increases with x. continuously. But for the case of ΔT_L = 16 K, at x ≈ 0.0075 m, the slope of (d(Nu)/dx) indicating that the location of T* is close to the wall. For ΔT_L = 20 K Nu increases with x up to a certain value of x (x ≈ 0.0075 m) beyond which the slope (d(Nu)/dx) becomes negative and Nu starts decreasing with increase in x.

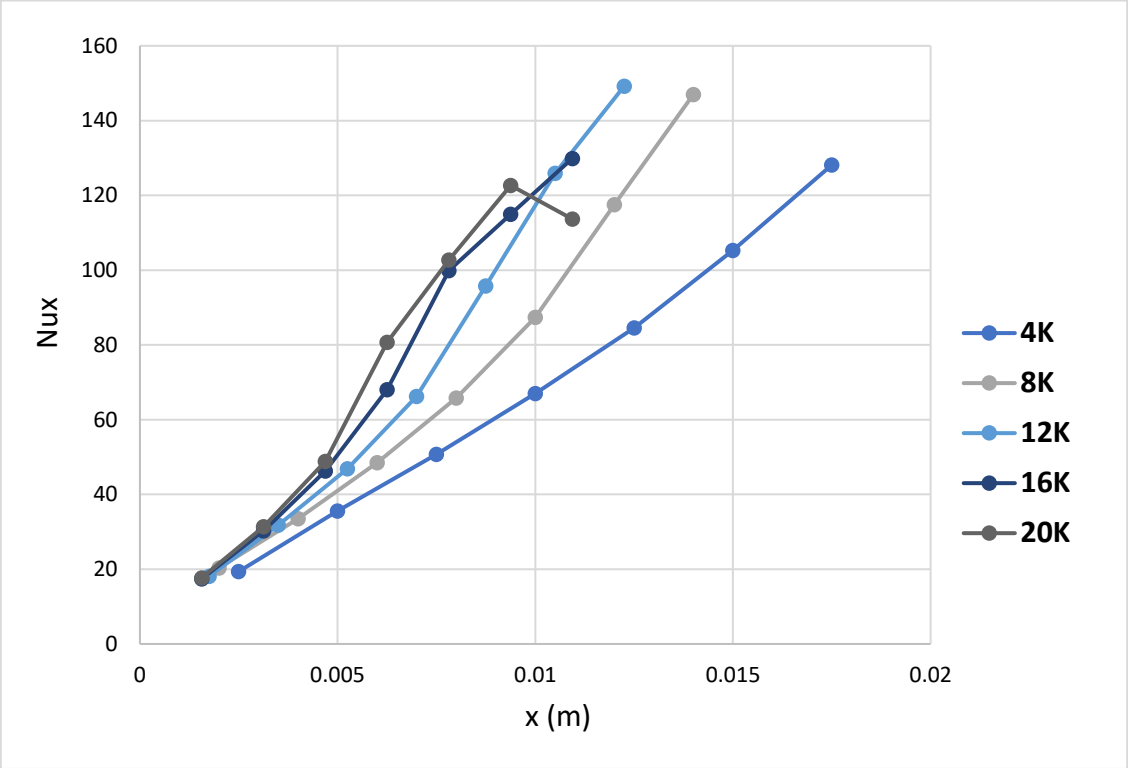

Fig. 34. Variation of Nu with x for five different values of of ΔT_L for water at 225 bars for mixed convection with parabolic wall temperature variation

The variation of Nu with x is shown in Figure 35 for 235 bar pressure. The nature of variation of Nu is similar to the case of 225 bar pressure except that for ΔT_L = 20 K Nu remains constant with respect to x beyond x ≈ 0.00115 m.

The influence of the type of variation of wall temperature on the Nusselt number is shown in Figure 36, where Nu is plotted against x for both linear wall temperature case and the parabolic wall temperature case, for two different values of ΔT_L, namely, ΔT_L = 4 K, for which T* does not lie within the boundary layer and ΔT_L = 16 K for which T* lies within the boundary layer. It can be seen from this plot that when T* does not lie within the boundary layer, Nu is practically the same for both the linear wall temperature variation and the parabolic wall temperature variation, up to a certain value of x (x≈ 0.01), beyond which Hu is higher for the parabolic wall temperature case. For the case when ΔT_L = 16 K, Nu for the linear wall temperature case increases with x up to a certain value of x ≈ 0.0125 m and is higher than that for the parabolic wall temperature case and then it becomes constant. But for the parabolic wall temperature case Nu continuously increases with x, with the result at x ≈ 0.0125, NU will be same for both the type of wall temperature variations and beyond this value of x, the parabolic wall temperature case gives higher value of Nu at any x than the linear wall temperature case.

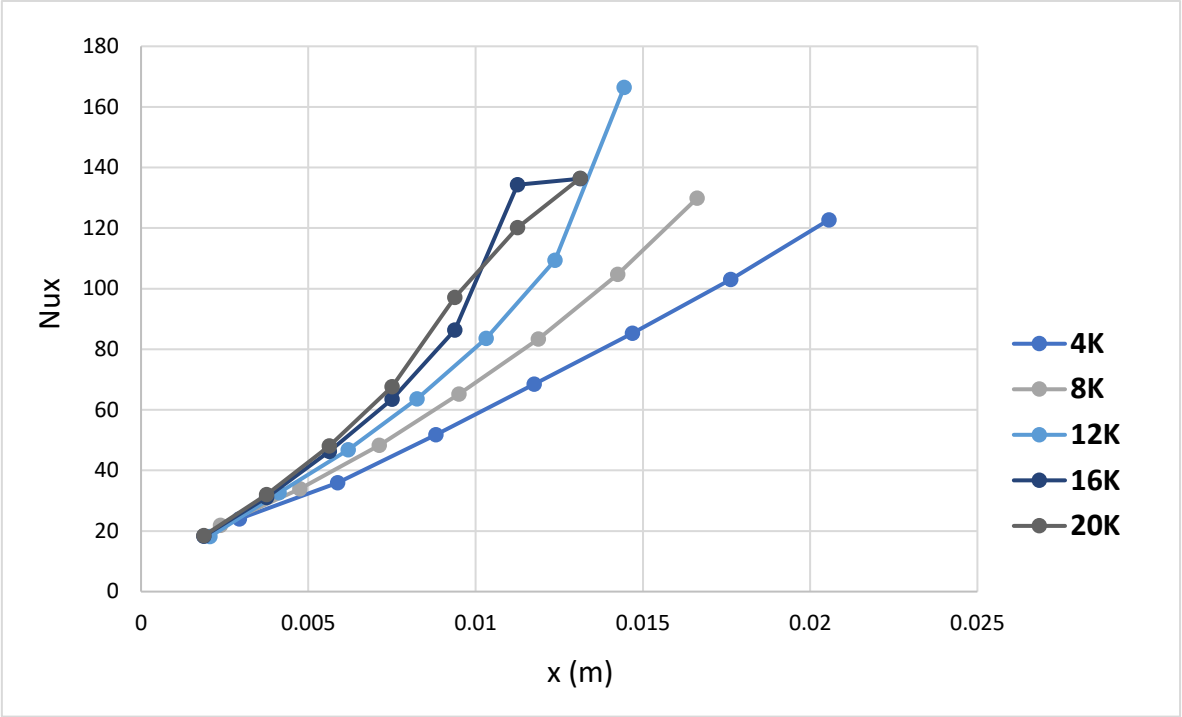

Fig. 35. Variation of Nu with x for five different values of of ΔT_L for water at 235 bars for mixed convection with parabolic wall temperature variation

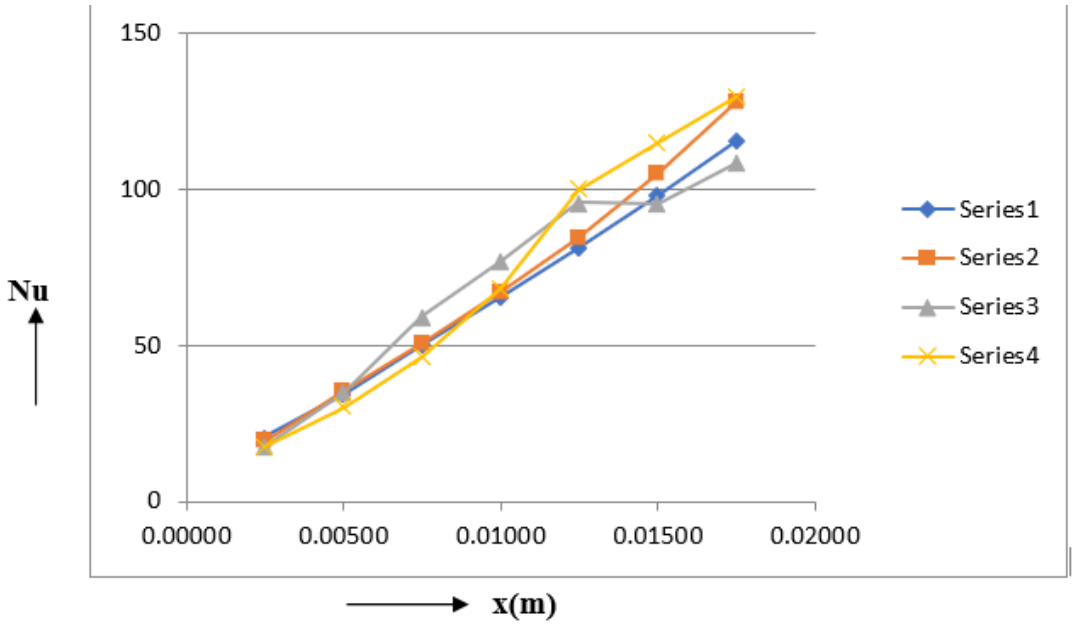

Series 1: ΔT_L = 4 K, Linear wall temperature
Series 2: ΔT_L = 4 Parabolical temperature
Series 3: ΔT_L = 16 K, Linear wall temperature
Series 4: ΔT_L = 16 K, Parabolic wall temperature

Fig. 36. Variation of Nu with x for two values of ΔT_L for 225 bar pressure for linear wall temperature and parabolic wall temperature cases

3.1.4 Correlations for mixed convection for linear wall temperature case and for parabolic wall temperature case

Two correlations to evaluate the Nusselt numbers for mixed convection are proposed based on numerical predictions, using multiple regression analysis. One correlation is for the case of linear wall temperature variation and the other for parabolic variation of wall temperature. The form of correlation is based on the recommendations of Ghorbani and Gajjar [23] who have recommended that all the propertry ratios, namely, ρ*, μ*, k* and c_p* should be taken into account in the correlation. Using multiple regression analysis and using 70 data points, the correlation for mixed convection from vertical flat plate with linear wall temperature is given by

$$\mathbf{(Nu_{ml})_c} = 0.575(Ra_x)^{0.184}\ (Re_x)^{0.161}(\rho^*)^{-0.865}\left(c_p^*\right)^{0.283}(\mu^*)^{0.864}(k^*)^{0.137} \quad (6)$$

with maximum deviation being ± 10 percent.and R^2 value of 0.996.The deviation of all data points with respect to Eq. (6) is shown in Figure 37.

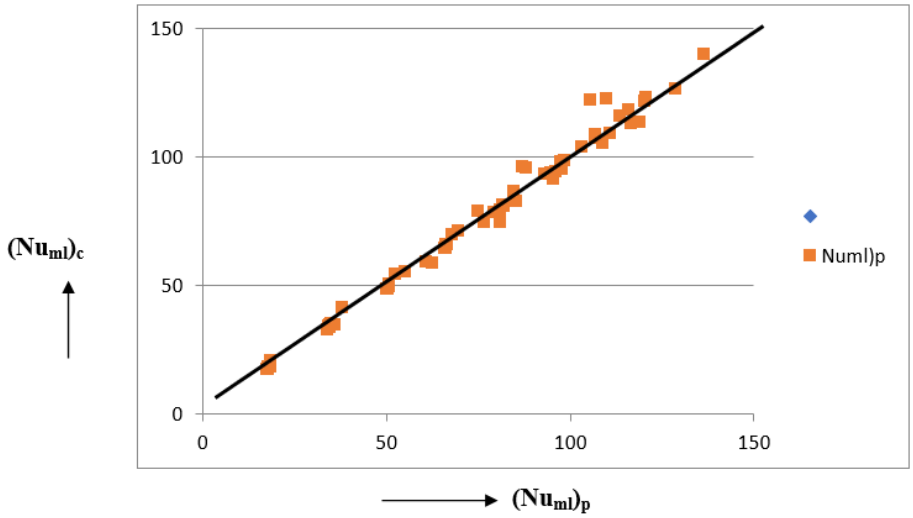

Fig. 37. Comparison between Nusselt number calculated using Eq. (6), $(Nu_{ml})_c$ and predicted Nusselt number, $(Nu_{ml})_p$ for linear wall temperature variation

Similarly, the correlation for Nusselt number for mixed convection with parabolic wall temperature is given by

$$(Nu_{ml})_c = 1.455(Ra_x)^{0.184}\ (Re_x)^{0.11}(\rho^*)^{0.213}\left(c_p^*\right)^{0.978}(\mu^*)^{-2.065}(k^*)^{0.317} \quad (7)$$

with maximum deviation being ± 15 percent.and R^2 value of 0.992.The deviation of all data points with respect to Eq. (7) is shown in Figure 38.

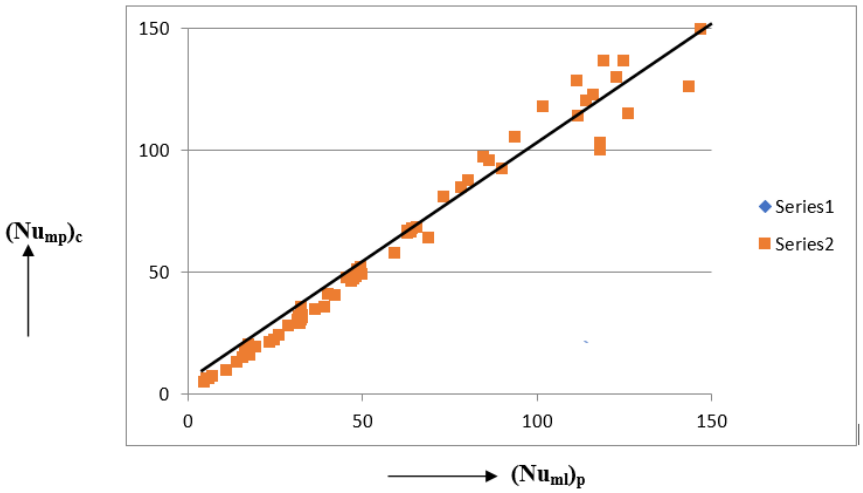

Fig. 38. Comparison between Nusselt number calculated using Eq. (6), $(Nu_{mp})_c$ and predicted Nusselt number, $(Nu_{ml})_p$ for paravbolic wall temperature variation

4. Conclusions

The problem of free and mixed convection heat transfer from a plane non isothermal vertical surface to supercritical water has been carried out for 225 bar and 235 bar pressures. The variation of all the properties of the fluid is taken into account by fitting polynomials using NIST property data. The numerical method employed for the present investigation is first validated with corresponding experimental data and it is found that numerical results are in good agreement with experimental values, the maximum deviation not exceeding $\pm$ 15 %. Two types of wall temperature variations namely linear variation and parabolic variation of wall temperature are chosen for investigation.

Based on the numerical predictions the following conclusions can be drawn

i. In all the cases studied for both linear variation and parabolic variation of wall temperature, the Nusselt number increases with increase in distance along the plate.
ii. The variation of *Nu* is found to be smooth for those cases for which T^* does not lie within the boundary layer, whereas for cases when T^* lies within the boundary layer there is distortion in the plot of Nu_x versus x. The distortion in the plot of Nu_x is found to occur for those cases for which the pseudo critical temperature lies within the boundary layer. The slope of $\frac{d\beta}{dT}$ changes sign across T^* and this influences the buoyancy force, which in turn affects the temperature gradient at the wall and hence the Nusselt number. This effect will persist up to wall temperatures several degrees higher than the pseudocritical temperature.
iii. The velocity profiles for the cases for which T^* does not lie within the boundary layer are found to be smooth, whereas for cases for which T^* lies within the boundary layer, the velocity profiles get distorted at locations where $T \approx T^*$. This distortion influences both the velocity gradient and the temperature gradient at the wall, thereby affecting the drag coefficient and the wall heat flux.

Based on the predictions, four correlations have been proposed. Two correlations for free convection [one for linear wall temperature variation and another for parabolic wall temperature

variation] and two for mixed convection. These correlations give Nusselt numbers which agree with actual predictions and deviation does not exceed $\pm$ 10 % for free convection with linear wall temperature, ± 11 % for free convection with parabolic wall temperature variation, $\pm$ 10 % for mixed convection with linear wall temperature variation and $\pm$ 15 % for mixed convection with parabolic wall temperature variation.

Acknowledgement
This research was not funded by any grant.

References

[1] Schlosky, Kevin M. "Supercritical phase transitions at very high pressure." *Journal of chemical education* 66, no. 12 (1989): 989. https://doi.org/10.1021/ed066p989
[2] Zonta, Francesco, and Alfredo Soldati. "Effect of temperature dependent fluid properties on heat transfer in turbulent mixed convection." *Journal of heat transfer* 136, no. 2 (2014). https://doi.org/10.1115/1.4025135
[3] Polyakov, A. F. "Heat transfer under supercritical pressures." In *Advances in heat transfer*, vol. 21, pp. 1-53. Elsevier, 1991. https://doi.org/10.1016/S0065-2717(08)70333-2
[4] Linstorm, P. "NIST chemistry webbook, NIST standard reference database number 69." *J. Phys. Chem. Ref. Data, Monograph* 9 (1998): 1-1951.
[5] Fritsch, C. A., and R. J. Grosh. "Free convective heat transfer to supercritical water experimental measurements." (1963): 289-293. https://doi.org/10.1115/1.3686108
[6] Hasegawa, Shu, and Keisuke Yoshioka. "An analysis for free convective heat transfer to supercritical fluids." In *International Heat Transfer Conference Digital Library*. Begel House Inc., 1966.
[7] KATo, Hiroharu, Niichi NISHIWAKI, and Masaru HIRATA. "Studies on the Heat Transfer of Fluids at a Supercritical Pressure: 1st Report, A Proposition of Reference Values of Thermal Properties and Experiments with Supercritical Carbon-Dioxide." *Bulletin of JSME* 11, no. 46 (1968): 654-663. https://doi.org/10.1299/jsme1958.11.654
[8] Nishkawa, Kaneyasu, and Takehiro Ito. "An analysis of free-convective heat transfer from an isothermal vertical plate to supercritical fluids." *International Journal of Heat and Mass Transfer* 12, no. 11 (1969): 1449-1463. https://doi.org/10.1016/0017-9310(69)90027-1
[9] Nowak, Edwin Stanislaus, and A. K. Konanur. "An analytical investigation of free convection heat transfer to supercritical water." (1970): 345-350. https://doi.org/10.1115/1.3449669
[10] Seetharam, T. R., and G. K. Sharma. "Numerical predictions of free convective heat transfer from vertical surfaces to fluids in the near-critical region." In *4th National Heat and Mass Transfer Conference*, pp. 273-279. 1978.
[11] Seetharam, T. R., and G. K. Sharma. "Free convective heat transfer to fluids in the near-critical region from vertical surfaces with uniform heat flux." *International Journal of Heat and Mass Transfer* 22, no. 1 (1979): 13-20. https://doi.org/10.1016/0017-9310(79)90093-0
[12] Seetharam, T. R., and G. K. Sharma. "HEAT TRANSFER BY TURBULENT FREE CONVECTION FROM A PLANE VERTICAL SURFACE TO NEAR-CRITICAL CARBON-DI-OXIDE." In *International Heat Transfer Conference Digital Library*. Begel House Inc., 1982. https://doi.org/10.1615/IHTC7.3330
[13] Graham, R. W., R. J. Simoneau, and J. C. Williams III. *Velocity and temperature profiles in near critical nitrogen*. No. NASA-TM-X-52988. 1971.
[14] Seetharam, T. R., K. N. Seetharamu, Girish Kumar Sharma, and Saravanan Venkatesh. "Laminar forced and mixed convection heat transfer from a plane vertical isothermal surface to near-critical carbon dioxide." *International Journal of Heat and Mass Transfer* 59 (2013): 393-406. https://doi.org/10.1016/j.ijheatmasstransfer.2012.12.034
[15] Teymourtash, Ali Reza, Danyal Rezaei Khonakdar, and Mohammad Reza Raveshi. "Natural convection on a vertical plate with variable heat flux in supercritical fluids." *The Journal of Supercritical Fluids* 74 (2013): 115-127. https://doi.org/10.1016/j.supflu.2012.12.010
[16] Teymourtash, Ali Reza, and Majid Ebrahimi Warkiani. "Natural convection over a non-isothermal vertical flat plate in supercritical fluids." *Scientia Iranica* 16, no. 6 (2009).
[17] Basha, Hussain, G. Janardhana Reddy, and N. S. Venkata Narayanan. "Thermodynamic analysis of natural convection supercritical water flow past a stretching sheet using an equation of state approach." *Canadian Journal of Physics* 99, no. 3 (2021): 185-201. https://doi.org/10.1139/cjp-2019-0384
[18] Basha, Hussain, G. Janardhana Reddy, NS Venkata Narayanan, and Mikhail A. Sheremet. "Analysis of supercritical free convection in Newtonian and couple stress fluids through EOS approach." *International Journal of Heat and Mass Transfer* 152 (2020): 119542. https://doi.org/10.1016/j.ijheatmasstransfer.2020.119542

[19] Basha, Hussain, G. Janardhana Reddy, and NS Venkata Narayanan. "Heat Transfer Characteristics of Nitrogen in Supercritical Region Using Redlich-Kwong Equation of State." *International Journal of Chemical Reactor Engineering* 17, no. 10 (2019). https://doi.org/10.1515/ijcre-2018-0279
[20] Redlich, Otto, and Joseph NS Kwong. "On the thermodynamics of solutions. V. An equation of state. Fugacities of gaseous solutions." *Chemical reviews* 44, no. 1 (1949): 233-244. https://doi.org/10.1021/cr60137a013
[21] Churchill, Stuart W., and Humbert HS Chu. "Correlating equations for laminar and turbulent free convection from a vertical plate." *International journal of heat and mass transfer* 18, no. 11 (1975): 1323-1329. https://doi.org/10.1016/0017-9310(75)90243-4
[22] Ghorbani-Tari, Saeed, and Afshin J. Ghajar. "Improved free convective heat-transfer correlations in the near-critical region." *AIAA journal* 23, no. 10 (1985): 1647-1649. https://doi.org/10.2514/3.9144